FINITE ELEMENT BASED CONVECTIVE RESPONSE ANALYSIS OF GROUND SUPPORTED RECTANGULAR LIQUID CONTAINERS

A Thesis

Submitted by

SRIKANTA SING
Class Roll No: 001710402004
Exam Roll No: M4CIV19009

In partial fulfillment of the requirements
for the award of the degree of

Master of Engineering
In
Civil Engineering
(Structural Engineering)

Under the Guidance of
DR. KALYAN KUMAR MANDAL

Department of Civil Engineering
Jadavpur University
Kolkata-700032
May-2019

DEPARTMENT OF CIVIL ENGINEERING
FACULTY OF ENGINEERING AND TECHNOLOGY
JADAVPUR UNIVERSITY
KOLKATA – 700 032

CERTIFICATE OF RECOMMENDATION

This is to certify that the thesis entitled, "**FINITE ELEMENT BASED CONVECTIVE RESPONSE ANALYSIS OF GROUND SUPPORTED RECTANGULAR LIQUID CONTAINERS**" submitted by **SRIKANTA SING**, Class Roll No.001710402004, Exam. Roll No. M4CIV19009, Registration No. 119655 of 2012-2013 in partial fulfillment of the requirements for the award of Master of Engineering degree in Civil Engineering with specialization in "Structural Engineering" at Jadavpur University, Kolkata is an authentic work carried out by him under my supervision and guidance.

I hereby recommend that the thesis be accepted in partial fulfillment of the requirements for awarding the degree of **"Master of Engineering in Civil Engineering (Structural Engineering)"**.

Dr. Kalyan Kumar Mandal
Associate Professor
Department of Civil Engineering
Jadavpur University
Kolkata- 700032

Countersigned by

Dr. Dipankar Chakravorty
Head of the Department
Department of Civil Engineering
Jadavpur University
Kolkata- 700032

Prof. Chiranjib Bhattacharjee
DEAN, FET
Jadavpur University
Kolkata- 700032

DEPARTMENT OF CIVIL ENGINEERING
FACULTY OF ENGINEERING AND TECHNOLOGY
JADAVPUR UNIVERSITY
KOLKATA – 700 032

CERTIFICATE OF APPROVAL

This thesis paper is hereby approved as a credible study of an engineering subject carried out and presented in a manner satisfactorily to warrant its acceptance as a pre-requisite for the degree for which it has been submitted. It is understood that, by this approval the undersigned do not necessarily endorse or approve any statement made, opinion expressed or conclusion drawn therein but approved the thesis paper only for the purpose for which it is submitted.

Committee of Thesis Paper Examiners

_____
Signature of Examiner

_____
Signature of Examiner

DECLARATION

I, Srikanta Sing, Master of Engineering in Civil Engineering (Structural Engineering), Jadavpur University, Faculty of Engineering & Technology, hereby declare that the work being presented in the thesis work entitled, "**Finite element based convective response analysis of ground supported rectangular liquid containers"** is authentic record of work that has been carried out at the Department of Civil Engineering, Jadavpur University, Kolkata under the guidance of Dr. Kalyan Kumar Mandal, Associate Professor, Department of Civil Engineering, Jadavpur University. The work contained in the thesis has not yet been submitted in part or full to any other university or institution or professional body for award of any degree or diploma or any fellowship.

Place: Kolkata
Date:

Srikanta Sing
Class Roll No: 001710402004
Exam Roll No: M4CIV19009
Regist. No: 119655 of 2012-2013

ACKNOWLEDGEMENT

I gratefully acknowledge the resourceful guidance, active supervision and constant encouragement of our reverent Associate Professor **Dr. Kalyan Kumar Mandal** of the Department of Civil Engineering, Jadavpur University, Kolkata, who despite his other commitments could find time to help me in bringing this thesis to its present shape. I do convey my sincere thanks and gratitude to him.

I also thankfully acknowledge my gratefulness to all Professors and staffs of Civil Engineering Department, Jadavpur University, Kolkata, for extending all facilities to carry out the present study.

I also thankfully acknowledge the assistance and encouragement received from my family members, friends and others during the preparation of this thesis.

Place: Kolkata
Date:

Srikanta Sing
Class Roll No: 001710402004
Exam Roll No: M4CIV19009
Regist. No: 119655 of 2012-2013

ABSTRACT

In the present study, the hydrodynamic pressure exerted by the fluid on walls of rectangular water tanks, due to horizontal excitations, is investigated by pressure based finite element method. The tank is considered to be two dimensional and base of tank and walls are assumed as rigid. The fluid with in the tank is considered as inviscid and fluid motion is irrotational. Galerkin approach is used for finite element formulation of weave equation. Newmark's average integration method which is unconditionally stable is used to obtain the response in time domain. The present algorithm also includes the compressibility of water in the reservoir.

The efficacy of the present algorithm has been demonstrated through numerous examples. The convective time period decreases with the increase of height to length ratio. The convective hydrodynamic pressure at free surface depends on length of container and remains same for all height of tank. However, this hydrodynamic pressure at the base and mid height of tank wall depends both on length and height of tank. The distribution of convective pressure is concentrated near the free surface for tank with comparatively lower height. However, the convective hydrodynamic distributed over the entire liquid for comparatively higher tank length. The sloshed displacement at the free surface depends on length and independent of height of tank. The sloshed displacement at the free surface increases with the increase of tank length.

KEYWORDS: *Compressibility of water, Finite element method, Convective Hydrodynamic Pressure, Fundamental time period, Newmark's integration*

LIST OF SYMBOLS

Symbols	Description
a	Acceleration of excitation
α	Acoustic weave speed
C_P	Hydrodynamic pressure coefficient
g	Gravitational acceleration
h	Height of fluid in tank
L	Length of the tank
ρ	Mass density of fluid
N_t	No of time steps
N_h	Nos. of horizontal division of mesh
N_v	Nos. of vertical division of mesh
P_c	Convective hydrodynamic Pressure
T	Time period of excitation
T_c	Convective time period
C_c	Convective time period coefficient
Q_{cw}	Convective pressure coefficient on wall
Q_{cb}	Convective pressure coefficient on base
σ	Total stress
μ	viscosity
u	Velocity component along x-axis
v	Velocity component along y-axis
F_x	Force component along x-axis
F_y	Force component along y-axis
ω	circulation frequency of vibration

CONTENTS

LIST OF FIGURES

LIST OF TABLES

CHAPTER 1

INTRODUCTION

1.1 General

Liquid container structures have become very popular during recent decade. This is one of the critical lifeline structures. Liquid containing structures are used for sewage treatment and storage of water, petroleum products, oxygen, nitrogen, high-pressure gas, liquefied natural gas (LNG), liquefied petroleum gas (LPG), etc. There are many types of fluid container depending on the construction material, volume, and storage condition. Liquid container can be made by steel or concrete. Due to extreme damages on steel tank, the concrete storage tanks are generally used nowadays. Reinforced Concrete (RC) is used in environmental engineering structures such as water reservoirs and sewage treatment tanks. Concrete tanks are efficient structural systems since they can be easily formed in different sizes to meet the requirements. Rectangular tanks are usually preferred because rectangular tanks are more efficient and easier to be separated into sub-tanks for different purposes. Container can also be classified as Ground supported container and Elevated container. It should be noted that the ground supported containers are more vulnerable structure and they have suffered considerable damage during earthquake because the accurate prediction of seismic behavior is not possible.

Water tanks should provide services for the emergency response of a community after an earthquake. If these structures fail during earthquake the citizen will fall in big problem because shortage of water or difficulty in putting out fires. This is why Liquid container should be designed in such a way that they can withstand earthquake loading without any structural damage. It should be noted that the seismic design of liquid storage tanks requires knowledge of fluid-structure interaction, natural frequencies, and hydrodynamic pressure distribution on the walls, resulting forces and moment as well as the sloshing of the contained liquid. In other word, hydrodynamic forces exerted by liquid on tank wall should be considered in the analysis in addition to hydrostatic forces.

When a tank containing liquid vibrates, the liquid exerts impulsive and convective hydrodynamic pressure on the tank wall and the tank base in addition the hydrostatic pressure. Under

earthquake loading, tank walls and liquid are subjected to horizontal acceleration and the total liquid mass gets divided into two parts, impulsive mass and convective mass. In the lower region of the tank, the liquid behaves like a mass that is rigidly connected to the tank walls and base. This mass is termed as impulsive liquid mass which accelerates along with the wall and base. This impulsive mass induces impulsive hydrodynamic pressure on the tank walls. Similarly, in the upper region of the tank, the liquid mass is not rigidly connected to the tank walls. This liquid mass undergoes sloshing motion. This mass is termed as convective liquid mass and exerts convective hydrodynamic pressure on the tank walls and base.

1.2 Objective

The objective of this study is, to develop a 2D finite element algorithm for obtaining convective responses of liquid within in the tank of different sizes.

CHAPTER 2

LITERATURE REVIEW

2.1 General

To provide a detailed review of the literature related to the dynamic analysis of liquid storage tank in it's entirely would be difficult to address in this chapter. A brief review of previous studies about dynamic analysis of liquid storage tank is presented in this section which are related to the present study. This literature review focuses on recent contributions related to this work and past efforts most closely related to the needs of the present work.

2.2 Literature Review

Tung Y. (1994) studied the dynamic characteristics of rigidly supported upright circular cylindrical tanks containing two different liquids. He also determined the fundamental natural frequency, the associated mode of vibration and the hydrodynamic pressure which are affected by the interaction of the liquids. The liquid region was solved analytically using Rayleigh- Ritz procedure in combination with Lagrange's equation and the displacements of the tank wall were expanded by the vibration nodes of the cantilever beam. This paper presents that even though the fundamental natural frequency was quite sensitive to control the parameter liquid height to radius of tank, the distribution of the associated modal pressure is not.

Choun Y.S. and Yun C.B. (1996) investigated the effects of a bottom-mounted rectangular block of arbitrary size and location on the sloshing frequencies and mode shapes of the fluid in rectangular rigid tanks using the linear water wave theory considering the liquid into the tank was incompressible and inviscid with irrotational motion. The analysis method was verified by comparing the results with other methods, like ADINA program. The sloshing frequencies and mode shapes were expressed in terms of the reflection and transmission coefficients, which were determined by the continuity conditions of mass flux and energy flux along the common vertical boundaries of the fluid regions. The fluid was divided into three regions, like the velocity potentials were composed of those due to wall-induced waves, reflected waves on the wall and block, transmitted waves over the block and scattered waves by the block. It was concluded that (i) The

sloshing frequencies, in general, decrease due to the presence of the internal block; (ii) The sloshing modes, i.e. the wave surface elevations, increase in the vicinity of the block; (iii) The sloshing frequencies and mode shapes vary more sensitively in the case of broad tanks $(d/L < 0.5)$ with a tall block $(h/d > 0.5)$; (iv) When the block was placed near the wall, the pressure on the both sides of the block could be in the same direction toward the centre of the tank and a large hydrodynamic force could be exerted on the block.

Pal N.C. et al. (2001) carried out a 3D finite element analysis for numerical simulation on the sloshing response of liquid filled cylindrical rigid base container assuming the contained fluid was incompressible and inviscid, resulting in an irrotational flow field. The effects of sloshing were computed in the time domain using Newmark's time integration scheme. The finite element discretization of the complete fluid domain was made assuming fluid velocity potential as the nodal unknown. A sensor device was especially developed to record the free surface wave height for experimental work. Two types of elements, namely, eight nodded isoparametric quadrilateral axis symmetric ring elements and tri-linear brick elements, were employed to discretize the fluid in the three dimensional domain, depending on the tank geometry, with velocity potential (ϕ) as the nodal unknown. The result obtained from numerical solution was compared with experimental value to judge the accuracy.

Cho J.R, Lee H.W. and Ha S.Y (2005) discussed about the resonant sloshing response in 2-D baffle tank. They developed a test FEM program for the resonant sloshing analysis in frequency domain. The choice of the artificial damping coefficient was parametrically examined and the numerical accuracy was verified through the comparison with the available analytic solutions. Through the numerical analysis of sloshing frequency response with respect to the number, location and opening width of baffle, the sloshing damping characteristics by the baffle were parametrically investigated. They confirmed the validity of the artificial damping introduced into the kinematic surface condition to reflect the eminent dissipation effect in the resonant liquid sloshing.

Takabatake D, Sawada S, Yoneyama and Miura M. (2008) studied the effect of splitting wall as sloshing reduction device in a cylindrical tank. They performed shaking table experiments to examine the effect of the splitting wall assuming the tank model is stiff enough to ignore the deformation of tank wall. This paper suggests that splitting wall is effective to reduce the sloshing against the sinusoidal input motion. They also carried out numerical simulation based on the three

dimensional incompressible analysis method assuming the density of fluid is constant. The result obtained from numerical simulation was compared with the experimental value to judge the accuracy.

Wei W, Junfeng L. and Tianshu .W (2008) discussed the modal analysis of liquid sloshing with different contact line boundary conditions using FEM. They established a finite element method (FEM) for liquid sloshing modal analysis. Surface tension and three kinds of contact line boundary conditions, namely, free-end, pin-end and wetting boundary conditions, were taken into account. Sloshing damping caused by energy dissipation at the wall, in the interior fluid and at the contact line was calculated. Numerical results were compared with the analytical values and measurements. For the pin-end and free-end boundary conditions the differences between numerical value and analytical value are small.

Chen Y.G, Djidjeli K. and Price W.G. (2008) carried out the numerical simulation of liquid sloshing phenomena in partially filled containers. A thin artificial buffer zone was adopted near the tank ceiling and a linear combination of free surface dynamic and rigid wall boundary conditions were imposed inside the buffer zone. This investigation demonstrated that no special treatment is needed to describe the free surface, because a two-fluid approach based on a level set method was used to solve the Reynolds-averaged Navier–Stokes (RANS) equations in both water and air regions and the inter-face is treated as a variation of the fluid properties. All the boundary conditions adopted were those usually accepted in solutions of Navier–Stokes or Euler equations. Sloshing in a rectangular tank excited by a horizontal harmonic motion was assessed numerically at different filling levels and excitation frequencies. The dependency of numerical solution on grid resolution, time step size and the interface thickness were investigated. Further, numerical tests were conducted for a rectangular tank with both 45L and 60L chamfered ceiling corners subject to a harmonic rolling motion.

Eswaran M, Saha U.K. and Maity D. (2008) discussed about the effect of baffles on a partially filled cubic tank. In this paper, sloshing waves were analyzed for baffled and un-baffled tanks. Numerical simulations were carried out based on volume of fluid (VOF) techniques with arbitrary Lagrangian–Eulerian (ALE) formulation which adopts the displacement of solid, the pressure and displacement in the fluid as variables to model the coupled system. The response of the coupled system was obtained by using the well-known software ADINA, which offers efficient fully

coupled fluid–structure interaction capabilities by finite element method. The results obtained were compared with the available experimental data to demonstrate the reduction of sloshing effects in fluid model.

Mitra S. and Sinhamahapatra K.P. (2008) carried out the 2D simulation of fluid-structure interaction using finite element method. The equations of motion of the fluid, considered inviscid and compressible, were expressed in terms of the pressure variable alone. The solution of the coupled system was accomplished by solving the two systems separately with the interaction effects at the fluid–solid interface enforced by an iterative scheme. Non-divergent pressure and displacement were obtained simultaneously through iterations. The Galerkin weighted residual method-based FE formulation and the iterative solution procedure were explained in detail followed by some numerical examples. Numerical results were compared with the existing solutions to validate the code for sloshing with fluid–structure coupling.

Idelsohn S, Torrecilla M.M. and Onate E. (2009) studied the Multi-fluid flows with the Particle Finite Element Method. The Particle Finite Element Method based on finite element shape functions was used to solve the continuous fluid mechanics equations in the case of heterogeneous density. . To evaluate the external applied forces to each particle, the incompressible Navier Stokes equations were solved at each time step using a Lagrangian formulation. All the information in the fluid is transmitted via the particles. All kinds of density heterogeneous fluids and multiphase flows with internal interfaces including or not free surfaces, breaking waves and fluid separations may were solved with this methodology.

Rebouillat S. and Liksonov D. (2009) discussed about the fluid–structure interaction in partially filled liquid containers. They used different type of numerical approaches to predict the sloshing wave amplitude, frequency, pressure exerted on the walls and the effect of sloshing on the stability in the container environment. They concerned primarily finite-elements and finite-differences methods applied to Euler or Lagrangian fluid and solid domains, as well as the smoothed particle method. Issues related to modeling the free-surface of the fluid, fluid–solid interface and to numerical coupling were exposed. Results obtained by various numerical methods were discussed in comparison with experimental results, where possible. Applications of sloshing models in naval, aerospace and other industries were described and discussed.

Ming P.J. and Duan W.Y. (2010) carried out the numerical simulation of sloshing in rectangular tank with VOF based on unstructured grids. They presented a new method for sloshing simulation in a sway tank, in which the two phase interface was treated as a physical discontinuity, which could be captured by a well-designed high order scheme. Based on Normalized Variable Diagram (NVD), a high order discretization scheme with unstructured grids was realized; together with a numerical method for free surface flow with a fixed grid. This method was implemented in an in-house code General Transport Equation Analyzer (GTEA) which is an unstructured grids finite volume solver. The present method was first validated by available analytical solutions. A simulation for a 2-D rectangular tank at different excitation frequencies of the sway was carried out. A comparison with experimental data in literature and results obtained by commercial software CFX shown that the sloshing load on the monitor points agrees well with the experimental data, with the same grids, and the present method gives better results on the secondary peak. It was shown that the present method can simulate the free surface overturning and breakup phenomena.

Pal P. and Bhattacharyya S.B (2010) discussed about the Sloshing in partially filled liquid 2-D containers. They developed a mesh less formulation to compute the nonlinear sloshing amplitude of liquid in liquid-filled prismatic containers subjected to sinusoidal base excitation. Mesh less local Petrov–Galerkin (MLPG) method was used for computing the nonlinear sloshing response of liquid in a two-dimensional rigid prismatic tank. At every instant of time, velocity potential was computed at each node and the nodal positions were updated. A local symmetric weak form (LSWF) for nonlinear sloshing of liquid was developed, and a truly mesh less method, based on LSWF and moving least squares (MLS) approximation, was presented for the solution of Laplace equation with the requisite boundary conditions. An experimental set-up was also designed to study the behavior of liquid sloshing in partially filled prismatic tank. The resulting slosh heights for various excitation frequencies and amplitudes were compared with the data obtained from the numerical studies. This paper suggests that, the numerical results are close to that obtained experimentally and little variations in the data are due to ineptness of the experimental set-up and the input parameters.

Faltinsen O.M and Timokha A.N (2010) discussed about the natural sloshing frequencies and modes in a rectangular tank with a slat-type screen. Employing the linear sloshing theory and domain decomposition method, they constructed an accurate analytical approximation of the natural sloshing modes in a rectangular tank with a slat-type screen at the tank middle. Two-dimensional

irrotational flow of an ideal incompressible liquid was assumed. Analyzing this solution they established a complex dependence of the natural sloshing frequencies on the solidity ratio, the number of submerged screen gaps, the liquid depth, and the position of perforated openings relative to the mean free surface. Results were compared with experimental data. Natural surface wave profiles were discussed in the context of a jump of the velocity potential at the screen and the local inflow component to the screen.

Yuan C. and Xianlong J. (2010) studied the dynamic response of flexible container during the impact with ground. They constructed a finite element model of the container to predict the dynamic response of the container. Water movement and sloshing in the container were modeled using the multi-material ALE method. Interaction between the container and the fluid was studied by the penalty method. Numerical results were compared with experiment data for the validation of the model and the approaches. This paper suggests that the shoulder of the container is the most vulnerable part during the impact and both the drop heights and the amount of water have great effects on the crashworthiness of the container.

Hasheminejad S.M and Aghabeigi M (2011) studied the transient sloshing in half full horizontal tank under lateral excitation. They developed a semi-analytical mathematical model to study the transient liquid sloshing characteristics in half-full horizontal cylindrical containers of elliptical cross section subjected to arbitrary lateral external acceleration. The problem solution was achieved by employing the linear potential theory in conjunction with conformal mapping, resulting in linear systems of ordinary differential equations which are truncated and then solved numerically by implementing Laplace transform technique followed by Durbin's numerical inversion scheme. A ramp-step function was used to simulate the lateral acceleration excitation during an idealized turning maneuver. The effects of tank aspect ratio, excitation input time, and baffle configuration on the resultant sloshing characteristics were examined. Limiting cases are considered and good agreements with available analytic and numerical solutions as well as experimental data were obtained.

Vakilaadsarabi A. and Miyajima M. (2012) investigated the sloshing of water reservoirs and tanks due to long period and long duration seismic motions. They used the computational fluid dynamic (CFD) simulation tool open FOAM (open field operation and manipulation) to study the effect of ground motions inside sloshing tank. An improved VOF method was used to assume an

accurate description of water displacement. Computational results were validated and compared to obtain some useful insight into the effect of period and duration of seismic motions on the sloshing phenomena in the water tank. It was concluded that the severity of sloshing and its dynamic pressure loads depend on the tank geometry, the depth of the liquid, the amplitude and the nature of the tank motions.

Wu C.H, Faltinsen O.M. and Chen B.F. (2012) carried out the numerical study of sloshing liquid in tanks with baffles by time-independent finite difference and fictitious cell method. The width of the baffle was very thin compared with the breadth length and the numerical technique used to capture the detailed flow phenomenon (vortex generation and shedding) around the baffle. In this paper, a time-independent finite difference scheme with fictitious cell technique was used to study viscous fluid sloshing in 2D tanks with baffles. The Navier–Stokes equations in a moving coordinate system were derived. The developed numerical model was rigorously validated by extensive comparisons with reported results. An experiment setup was also made to validate the present numerical sloshing results in a tank with baffles. The method was applied to a number of problems including impulsive flow past a flat plate, sloshing fluid in a 2D tank with a surface-piercing baffle, sloshing fluid in 2D tanks with bottom-mounted baffles. The effects of baffles on the resonant frequency were discussed.

Javanshir A, Elahi R. and Passandideh-fard M. (2013) carried out the numerical simulation of liquid sloshing with baffles in the fuel container. They developed a two dimensional numerical model to study viscous liquid sloshing in a tank with internal baffles. The model was validated by a comparison between the computational and experimental results for time dependent linear acceleration sloshing scenarios. The deformation of liquid – gas interface was modelled using the volume of fluid (VOF) method. The fluid flow equations describing the fluid sloshing in the container and the dynamic equation which describes the movement of the container were solved separately in two coupled programmes. In each time step of computations, the output of fluid program (forces and torque) were obtained and used as inputs for the dynamic program. The force and torque were applied to the body of container resulting in translational accelerations which are then used as an input to the fluid program. It was shown that the total kinetic energy of fluid that baffles have an important role to reduce the liquid sloshing in a container.

Jiang M.R., Ren B., Wang G.Y. and Wang Y.X (2013) investigated the hydro elastic effect on liquid sloshing in rectangular tanks. The conducted a sloshing experiment to study the hydro elastic effect in an elastic tank. For this purpose, a translational harmonic excitation was applied to a 2-D rectangular tank model. The lowest-order natural frequencies of the liquid in the tank were determined through the sweep test. The wave elevation and the sloshing pressure were obtained by changing the excitation frequency and the liquid depth. Then the characteristics and the variation of the elevation and the pressure were discussed. The results were compared with the experimental results and the theoretical calculations in a rigid tank. Their analysis indicates that, in the non-resonant cases, the elastic results, the rigid experimental results and the theoretical values are all close to each other. They concluded that under the resonant condition, the elastic experimental result is slightly smaller than the rigid one

Lin L, Sheng C.j, Ming.z. andGuo Q.T (2013) studied the two dimensional viscous numerical simulation of liquid sloshing in rectangular tank with/without baffles and comparison with potential flow solution. They developed a fluid model based on non-inertial reference system for the problem of liquid sloshing in rectangular tank with/without baffles. The accuracy of the numerical model was validated against available theoretical solutions, experimental data and numerical predictions by linear and non-linear potential flow models and different Navier–Stokes solvers. This paper suggests that the dissipative effects have significant influence on the sloshing responses in both non-baffled and baffled tanks.

Miao Y. and Wang S. (2013) investigated about the Small amplitude liquid surface sloshing process detected by optical method. They constructed a experimental set up to detect liquid surface sloshing wave excited by the instantaneous momentum. The sloshing parameters were determined by detecting the scattering light. The analytical expressions which include the relationship between optical intensity and liquid surface sloshing wave and the expressions of the wave length as well as amplitude were derived theoretically. Optical patterns corresponding to static and sloshing liquid surface were obtained experimentally. The sloshing variation process including rising and damping was achieved. Both rising and damping processes were variable exponentially. The rising and damping coefficients and maximum amplitude as well as wavelength of the sloshing wave were also measured experimentally.

Zhang Y.X. and Wan D.C (2014) carried out a Comparative study of MPS (moving particle semi-implicit) method and level-set method for sloshing flows. The numerical schemes of the MPS and level-set methods were outlined and two violent sloshing cases were considered. The computed results were compared with the corresponding experimental data for validation. The impact pressure and the deformations of free surface induced by sloshing were comparatively analyzed, and were in good agreement with experimental ones. Results proved that both the MPS and level-set methods are good tools for simulation of violent sloshing flows. However, the second pressure peaks as well as breaking and splashing of free surface by the MPS method were captured better than by the level-set method.

Jung J.H, Yoon H.S. and Lee C.Y. (*2015*) studied the effect of natural frequency modes on sloshing phenomenon in a rectangular tank. Liquid sloshing in two-dimensional (*2-D*) and three-dimensional (*3-D*) rectangular tanks was simulated by using a level set method based on the finite volume method. In order to examine the effect of natural frequency modes on liquid sloshing, they considered a wide range of frequency ratios ($0.5\ 3.2\ f_r \leq\leq 3.2$). The frequency ratio is defined by the ratio of the excitation frequency to the natural frequency of the fluid, and covers natural frequency modes from 1 to 5. When $f_r = 1$, which corresponds to the first mode of the natural frequency, it was shown that significant forces are generated by the liquid in the tank. The liquid flows are mainly unidirectional. Thus, the strong bulk motion of the fluid contributes to a higher elevation of the free surface. However, at $f_r = 2$, the sloshing is considerably suppressed, resulting in a calm wave with relatively lower elevation of the free surface, since the waves undergo destructive interference. At $f_r = 2$, the lower peak of the free surface elevation occurs. At higher modes of $f_r=3$. $f_r = 4$, the free surface reveals irregular deformation with nonlinear waves in every case. However, the deformation of the free surface becomes weaker at higher natural frequency modes. Finally, 3-D simulations confirm their 2-D results.

Xue M.A. and Lin P. (2015) carried out the numerical study of ring baffle effects on reducing violent liquid sloshing. They developed a three-dimensional (3-D) numerical model NEWTANK to study viscous liquid sloshing in a tank with internal baffles of different shapes and arrangements. The numerical technique named virtual boundary force (VBF) method was used to model the internal baffles with complex geometries. Laboratory experiments were conducted for non-linear sloshing in a rectangular tank with and without vertical baffle. The numerical model was validated

against the measured data together with other available theoretical solutions and numerical results for liquid sloshing under surge and pitch motions. Liquid sloshing in a 3D prismatic tank with different ring baffle arrangements (e.g., height, width, etc.) were further investigated under near-resonant excitations of surge and pitch motions. The fast Fourier transform (FFT) technique was used to identify the dominant response frequencies of the liquid system to external excitations. The effects of ring baffles on reducing violent liquid sloshing were investigated. Finally, a demonstration of liquid sloshing in the tank under six degree-of-freedom (DOF) excitations was presented.

Cheng X.D and Wen J.H (2015) discussed about the dynamic characteristics of liquid forced sloshing in a turning spherical tank with a spacer under low gravity. In this discussion, the static shape of the liquid surface was analyzed. By expanding the characteristic functions, the frequencies and velocity potential of liquid free-sloshing were derived. The governing equations and boundary conditions for the forced sloshing of liquid under the tank turning were established. The transverse force of liquid acting on the tank and the moment of force to the centre of the tank which is caused by the force of liquid acting on the spacer were given. Numerical results were compared with the ones of the spherical tank without a spacer. It was found that when a spacer is inserted in the tank, the sloshing frequency of liquid and the transverse force of liquid acting on the tank will decrease, but the moment of force to the centre of the tank which is caused by the force of liquid acting on the spacer will occur

Zhang H. and Wang Z. (2016) discussed about the attitude control and sloshing suppression for liquid-filled spacecraft in the presence of sinusoidal disturbance. The attitude regulation for a liquid-filled spacecraft in the presence of low frequency sinusoidal disturbance was considered in this paper. They modeled the liquid-filled spacecraft as a rigid body attached with a simple pendulum. A novel control scheme was proposed, which is composed of Active Disturbance Rejection Control (ADRC), Positive Position Feedback (PPF), Extended State Observer (ESO) and Singular Spectrum Analysis (SSA). The proposed approach could provide stabilization for the spacecraft, rejection for the disturbance, and active damping for the sloshing. Its effectiveness was validated by numerical simulations. A controller in the form of ADRC plus PPF was designed with estimated pendulum angle as PPF input. Simulation results illustrated the effectiveness of the presented approach. The design is useful not only for their presented application but also for others such as spacecraft with flexible structures.

Nan. M, Junfeng L. and Tianshu W. (2016) studied the equivalent mechanical model of large-amplitude liquid sloshing under time-dependent lateral excitations in low-gravity conditions. They proposed an equivalent mechanical model for large-amplitude liquid sloshing in partially filled spherical tanks subjected to lateral excitations. The hypothesis of liquid equilibrium position following equivalent gravity was first proposed, which means that the pendulum mass and rigid-attached mass block both move with equivalent gravity. A better simulation of large-amplitude liquid sloshing was shown by decomposing the large-amplitude motion of the liquid into bulk motion following the equivalent gravity and additional small-amplitude sloshing. The hypothesis, as well as the accuracy of the composite model, was verified by comparison with the CFD software in several numerical simulations.

Cho I.H and Kim M.H. (2016) investigated the effect of dual vertical porous baffles on sloshing reduction in a swaying rectangular tank. The effect of dual vertical porous baffles on the sloshing reduction inside a rectangular tank was investigated both theoretically and experimentally. The matched Eigen function expansion method was applied to obtain the analytic solutions in the context of linear potential theory with porous boundary conditions. The porosity effect was included through inertial and quadratic-drag terms. The theoretical prediction was then compared with a series of experiments conducted by authors with harmonically oscillated rectangular tank at various frequencies and baffle parameters. The measured data reasonably correlated with the predicted values. It was found that the dual vertical porous baffles can significantly suppress sloshing motions when properly designed by selecting optimal porosity, submergence depth, and installation position.

Su Y. and Liu Z.Y. (2016) discussed about the Numerical model of sloshing in rectangular tank based on Boussinesq type equations. They adopted the highly accurate Boussinesq type equations in terms of velocity potential for the simulation of sloshing phenomena in a two-dimensional rectangular tank. The fully nonlinear free surface conditions were used and linearized energy dissipation term was added into the dynamic free surface condition. The total velocity potential was divided into two parts: the particular solution and the rest which is calculated by the Boussinesq type model. Different filling levels of liquid in the tank were considered for the validation of the numerical model, including shallow water, intermediate water depth and finite water depth cases. The linear theory based on the superposition of Eigen modes corresponding to natural sloshing frequencies was introduced and compared with results calculated by linear theory

and results from literatures. This paper suggests that the numerical model based on Boussinesq type equations presents good performances in predicting the sloshing motions in rectangular tank with small excitation amplitude.

Boroomand B, Bazazzadeh S. and Zandi S.M. (2016) discussed on the use of Laplace's equation for pressure and a mesh-free method for 3d simulation of nonlinear sloshing in tanks. They presented a consistent 3D mesh-free method for the solution of free surface sloshing in tanks. In this method a linear summation of exponential basis functions (EBFs) was assumed as an approximation to the solution. The coefficients of the series were determined by a collocation technique used on a set of boundary nodes. These coefficients and the surface boundary nodes were updated through a time marching algorithm. Linear/non-linear 3D sloshing problems were solved in both rectangular and cylindrical basins. It was shown that the method may be used as an effective tool for 3D simulation of tanks with various shapes without the need for a huge number of domain/boundary elements for the discretization.

Chaudhari1 K., Bhilare B.L. and Patil G.R. (2017) studied the dynamic response of circular water tank with baffle walls. They considered two type of baffle walls i.e., vertical and ring baffle wall. The numerical study was done with the help of finite element model of tank fluid system using ANSYS software. It was concluded that baffle wall increases the performance of circular water tank during earthquake. They also carried out dynamic analysis for models with and without baffle wall and results were plotted.

Xue M.N, Zheng J, Lin P. and Yuan X. (2017) carried out the experimental study on vertical baffles of different configuration in suppressing sloshing pressure. The effectiveness of four types of the baffles in suppressing pressure was experimentally investigated under a wide range of forcing frequencies. The dynamic impact pressure variations alongside the central line of the tank wall and the baffle response to different excitation frequencies were measured for tanks without baffles and with immersed bottom-mounted vertical baffles, vertical baffles flushing with free surface, surface-piercing bottom-mounted vertical baffles and perforated vertical baffles, respectively. This paper suggests that the maximum impact pressure on the tank wall generally increases with decreasing the distance of the pressure sensor away from the free surface. They concluded that, the vertical baffle flushing with free surface is an more effective tool on reducing impact pressure comparing with the immersed bottom-mounted vertical baffle, especially near the first-mode natural frequency, in the

frequency range from $0.4\omega_1$ to $1.4\omega_1$ and effect of the perforated vertical baffle in suppressing sloshing pressure is more significant than that of the surface-piercing bottom-mounted vertical baffle, especially in high forcing frequency region. It was found that the first-mode natural frequency of liquid-tank is altered by the vertical baffles.

Iranmanesh A. and Passandideh-Fard M. (2017) carried out a 2D numerical study on suppressing liquid sloshing using a submerged cylinder. They proposed a two-dimensional numerical model to study the effect of a submerged cylinder on suppressing liquid sloshing in a moving container. The continuity and Navier-Stokes equations were solved along with an equation for the free surface advection. The Volume of Fluid (VOF) method was used to simulate the free-surface deformation. Two scenarios for the liquid sloshing were studied. In the first case, the liquid container was excited with a Constant Acceleration (CA). For the second case, the container was moved with a Single Oscillatory Excitation (SOE). The suppression rate of total kinetic energy of sloshing with the submerged cylinder for two scenarios were calculated and compared to the cases with free sloshing with no cylinder. For the first and second scenarios, using the submerged cylinder reduced the total kinetic energy of sloshing by 26.58% and 71.6%, respectively.

Sufyan M, Ngo L.C and Choi H.G. (2017) studied a dynamic adaptation method based on unstructured mesh for solving sloshing problems. They used a dynamic mesh-adaptation algorithm based on an unstructured mesh to solve sloshing problems. An implicit discretization method was employed to solve the incompressible Navier-Stokes equations; an assembled global matrix was generated using a dynamic compressed sparse row (CSR) method. The proposed algorithm was validated by comparing the simulation results with those of a non-adaptive method with respect to wall impact pressures and mass conservation. Numerical results showed that relative mass error strongly depends on mesh resolution near the interface. Results of adaptive simulations were found to be comparable with those of non-adaptive simulations only if a similar mesh resolution was used near the interface. Moreover, adaptive simulations were about two times faster than the non-adaptive ones. The effect of the adaptive zone and smoothing zone on the impact pressure was also examined for the proposed algorithm.

Liu D, Tang W, Wang J, Xue H. and Wang K. (2017) carried out a modelling of liquid sloshing using CLSVOF method and very large eddy simulation. They developed the new very large eddy simulation (VLES) model is developed in this paper to overcome some of the apparent

deficiencies of RANS and large eddy simulation (LES). Two filling levels, 18.3% and 43.7%, were considered in this analysis. Some complicated sloshing phenomena, including the plunging wave breaking, wave impact on the sidewall and the roof and the beating phenomenon were observed in these sloshing cases. The computational velocity fields, wave profiles and pressure data were compared with experimental results from Delorme and Souto Iglesias. The specific objectives were: to evaluate the performance of the CLSVOF method and VLES model for modelling of liquid sloshing; (ii) to investigate the influence of interface capturing method and turbulence model on sloshing simulation results.

Yu Y.M, Ma. N, Fan. C.M. and Gu. X.C. (2017) carried out experimental and numerical studies on sloshing in a membrane-type LNG tank with two floating type baffle plates. Sloshing with two floating plates in a membrane-type liquefied natural gas (LNG) tank was experimentally studied at three different filling rates under purely harmonic roll excitation. Their primary objective was to determine the performance of the suppressing device and of corresponding mechanisms. They concluded that the suppressing device can effectively damp the wave run up along the longitudinal bulkhead and the impact pressure acting on the bulkhead under the mild excitation amplitudes and, especially at the top of the tank. Furthermore, a numerical simulation based on a computational fluid dynamics (CFD) program was introduced to conduct an additional investigation. The accuracy of the numerical simulation was verified against experimental results by comparing the wave elevation and heave motion of two floating plates relative to the tank. The wave run up along the vertical side wall and the velocity field in the tank with floating plates were numerically evaluated and discussed as a supplement to obtain more dissipative mechanisms.

Cho I.H, Choi J.S. and Kim M.H. (2017) studied the Sloshing reduction in a swaying rectangular tank by a horizontal porous baffle. They used the MEEM (matched Eigen function expansion method) to obtain the analytic solution for the sloshing with porous horizontal baffle. A BEM (boundary element method) with the porous boundary conditions was also independently developed for double checking and the application to more general cases. Two baffle positions at the center and at both walls of a rectangular tank were considered for various porosities, lengths, and submergence depths. The theoretical prediction was then compared with a series of experiments conducted by authors using harmonically oscillated rectangular tank with various baffle porosities and submergence depths. The measured data reasonably correlate with the predicted values. It was

found that horizontal porous baffle installed at both tank walls significantly suppress violent resonant sloshing responses compared to one installed at the tank center.

Grotle E.L, Bihs. H. and Vilmar E. (2017) carried out the experimental and numerical investigation of sloshing under roll excitation at shallow liquid depths. They investigated sloshing at shallow-liquid depths in a rectangular container by using experimental and numerical methods. A motion platform was used to perform a prescribed periodic rotational motion to excite the liquid sloshing at a range of frequencies and filling levels. Simulated free-surface elevation was compared with the experimental results for a selection of cases. The wave mechanisms at the chosen fillings were studied by combining numerical methods and the experimental results. They concluded that the simulated free-surface elevation is in close agreement with experimental results inside the resonance zone, but at frequencies above the bifurcation point, with several overlapping waves, the deviation is increasing. The bifurcation point was determined for a range of filling levels through observation. This paper suggests that the complex interaction between the bottom, the lower layer and the wave influences the amount of dissipation before the wave hits the wall.

Adhikary R. and Mondal K.K. (2018) carried out the dynamic analysis of water storage tank with rigid block at bottom. They carried out both free vibration and forced vibration analysis for different sizes and positions of block at tank bottom. The water in the tank was considered to be linearly compressible as well as incompressible. They used a pressure based finite element method to simulate the dynamic behaviour of water in tanks. They concluded that the fundamental frequency of tank water decreases with increase of the block height. This paper also presents that increase in the pressure becomes insignificant after a certain value of the distance between the wall and the rigid block.

2.3 Critical Observations

Based on the review of literatures some critical observations are acknowledged. These observations are described below.

- Finite element analysis is recognized to be the one of the numerical tool for dynamic analysis of water tanks.

- The water within the tank is expressed by several variables such as displacement, velocity potential and pressure. Out of these variables, it is advantageous to model the fluid within the tank by pressure, as the number of degrees of freedom per node in this case reduced to one.
- In pressure based formulation, the number of unknown per node is only one. Thus it requires less storage place and computational time.
- In pressure based formulation, fluid satisfies the irritational condition automatically. Otherwise, a complicated condition has to be incorporated to satisfy the irrotanionality condition.
- For dynamic analysis of water tank, the water within the tank may be modeled either as compressible or incompressible fluid.
- Linear and nonlinear wave theory may be used to model the reservoir. However, for water with comparatively smaller depth linear wave theory is sufficient.
- At a certain limit of width to length ratio (*B/L*) the performance of tank in 2D and 3D are almost similar.
- It is important to consider both horizontal and vertical ground acceleration for overall seismic behavior of liquid storage tanks. However, the horizontal ground acceleration becomes more significant when the walls of tank are assumed to rigid.
- The free surface displacement of liquid depends on the tank aspect rations and the baffle within the tank. It also depends of the position, size and type of the baffle present in the tank.

2.4 Scope of Present Work

In order to realize the objective of the present work, the scope of the present research has been defined as follows:

- Development of pressure based *2-D* finite element formulation of water within the rectangular tank considering water to be compressible.
- Evaluation of hydrodynamic pressure on the tank walls for different sizes of containers.
- Evaluation of velocity and acceleration of water within the containers.
- Evaluation of sloshed displacement of the free surface of water.

CHAPTER 3

THEORITICAL FORMULATION

3.1 Theoretical Formulation

The state of stress for a Newtonian fluid is defined by an isotropic tensor as

$$\sigma_{ij} = -P\delta_{ij} + \sigma'_{ij} \tag{3.1}$$

Where σ_{ij} is total stress, σ'_{ij} is viscous stress tensor which depends only on the rate of deformation in such a way that the value becomes zero when the fluid is under rigid body motion or rest. The variable P is defined as hydrodynamic pressure whose value is independent explicitly on the rate of deformation and Δ_{ij} is kronecker delta. For isotropic linear elastic material, the most general from of σ'_{ij} is

$$\sigma'_{ij}=\psi\Delta\delta_{ij} + 2\mu D_{ij} \tag{3.2}$$

Where, μ and ψ are two material constants. μ is known as first co-efficient of viscosity or simply viscosity and $(\psi+2\mu/3)$ is second co-efficient of viscosity or bulk viscosity. D_{ij} is the rate of deformation tensor and is expressed as

$$D_{ij} = \frac{1}{2}\left(\frac{\partial v_i}{\partial y_j} + \frac{\partial v_j}{\partial x_i}\right) \qquad D = D_{11} + D_{22} + D_{33} \tag{3.3}$$

Thus, the total stress tensor becomes

$$\sigma_{ij} = -P\delta_{ij} + \psi\Delta\delta_{ij} + 2\mu D_{ij} \tag{3.4}$$

For compressible fluid, bulk viscosity (ψ+2μ/3) is zero. Thus, equation (3.4) becomes

$$\sigma_{ij} = -P\delta_{ij} - \frac{2\mu}{3}\Delta\delta_{ij} + 2\mu D_{ij} \tag{3.5}$$

If the viscosity of fluid is neglected, equation (3.5) becomes

$$\sigma_{ij} = -P\delta_{ij} \tag{3.6}$$

Generalized Navier-stokes equations of motion are given by

$$\rho_f \left(\frac{\partial v_i}{\partial t} + v_j \frac{\partial v_i}{\partial x_j}\right) = \frac{\partial \sigma_{ij}}{\partial x_j} + \rho_f B_i \tag{3.7}$$

Where B_i is the body force and ρ_f is the mass density of fluid. Substituting Eq. (3.6) in Eq. (3.7) the following relations are obtained.

$$\rho_f (\frac{\partial v_i}{\partial t} + v_j \frac{\partial v_i}{\partial x_j}) = \rho_f B_i - \frac{\partial P}{\partial x_i} \tag{3.8}$$

If *u* and *v* are the velocity components along x and y axes respectively, $f_x \; and \; f_y$ are the body forces along *x* and *y* direction respectively and if the convective terms are neglected, the equation of motion may be written as

$$\frac{1}{\rho_f}\frac{\partial P}{\partial x} + \frac{\partial u}{\partial t} = F_x \tag{3.9}$$

$$\frac{1}{\rho_f}\frac{\partial P}{\partial y} + \frac{\partial v}{\partial t} = F_y \tag{3.10}$$

Neglecting the body forces equation (3.9) and (3.10) become

$$\frac{1}{\rho_f}\frac{\partial P}{\partial x} + \frac{\partial u}{\partial t} = 0 \tag{3.11}$$

$$\frac{1}{\rho_f}\frac{\partial P}{\partial y} + \frac{\partial v}{\partial t} = 0 \tag{3.12}$$

The continuity equation of fluid in two dimensions is expressed as

$$\frac{\partial P}{\partial t} + \rho_f \alpha^2 (\frac{\partial u}{\partial x} + \frac{\partial v}{\partial x}) \tag{3.13}$$

Where, α is the acoustic wave speed in fluid. Now, differentiating equations (3.11) and (3.12) with respect to *x* and *y* respectively, the following relations are obtained.

$$\frac{1}{\rho_f}\frac{\partial^2 P}{\partial x^2} + \frac{\partial}{\partial x}\left(\frac{\partial u}{\partial t}\right) = 0 \tag{3.14}$$

$$\frac{1}{\rho_f}\frac{\partial^2 P}{\partial y^2} + \frac{\partial}{\partial y}\left(\frac{\partial v}{\partial t}\right) = 0 \tag{3.15}$$

Adding equations (3.14) and (3.15) the following expression is finally arrived.

$$\frac{1}{\rho_f}\frac{\partial^2 P}{\partial x^2}+\frac{1}{\rho_f}\frac{\partial^2 P}{\partial y^2}+\frac{\partial}{\partial x}\left(\frac{\partial u}{\partial t}\right)+\frac{\partial}{\partial y}\left(\frac{\partial v}{\partial t}\right)=0 \tag{3.16}$$

Differentiating equation (3.13) with respect to time, the following expression can be obtained.

$$\frac{\partial^2 P}{\partial t^2}+\rho_f \alpha^2\left\{\frac{\partial}{\partial x}\left(\frac{\partial u}{\partial t}\right)+\frac{\partial}{\partial y}\left(\frac{\partial v}{\partial t}\right)\right\}=0 \tag{3.17}$$

Thus from equation (3.16) and (3.17) one can find the following expression

$$\frac{1}{\rho_f}\frac{\partial^2 P}{\partial x^2}+\frac{1}{\rho_f}\frac{\partial^2 P}{\partial y^2}-\frac{1}{\rho_f \alpha^2}\frac{\partial^2 P}{\partial t^2}=0 \tag{3.18}$$

Simplifying the equation (3.18) the equation for compressible fluid may be obtained

$$\nabla^2 P(x,y,t)=\frac{1}{\alpha^2}\ddot{P}(x,y,t) \tag{3.19}$$

If the compressibility of fluid is neglected the equation (3.19) will be modified as

$$\nabla^2 P(x,y,t)=0 \tag{3.20}$$

The pressure distribution in the fluid domain may be obtained by solving equation (3.19) with the following boundary conditions. A typical geometry of tank-water system is shown in the figure 4.1

1) <u>At surface I</u>

Considering the effect of surface wave of the fluid, the boundary condition of the free surface is taken as

$$\frac{1}{g}\ddot{P}+\frac{\partial P}{\partial y}=0 \tag{3.21}$$

2) <u>At surface II</u>

At water-tank wall interface, the pressure should satisfy

$$\frac{\partial P}{\partial n}(0,y,t)=\rho_f a e^{i\omega t} \tag{3.22}$$

Where $ae^{i\omega t}$ is the horizontal component of the ground acceleration in which,ω is the circulation frequency of vibration and i=$\sqrt{-1}$, n is the outwardly directed normal to the element surface along the interface. ρ_f is the mass density of the fluid.

3) At surface III

This surface is considered as rigid surface and thus pressure should satisfy the following condition

$$\frac{\partial P}{\partial n}(x,0,t) = 0.0 \quad (3.23)$$

3.2 Finite Element Formulation

By using Galerkin approach and assuming pressure to be the nodal unknown variable, the discretized from equation (3.19) may be written as

$$\int_{\Omega} N_{rj}[\nabla^2 \sum N_{ri}P_i - \frac{1}{\alpha^2}\sum N_{ri}\ddot{P}_i]d\Omega = 0 \quad (3.24)$$

Where, N_{rj} is the interpolation function for the reservoir and Ω is the region under consideration.

Using Green's theorem equation (3.24) may be transformed to

$$-\int_{\Omega}[\frac{\partial N_{rj}}{\partial x}\sum\frac{\partial N_{ri}}{\partial x}P_i + \frac{\partial N_{rj}}{\partial y}\sum\frac{\partial N_{ri}}{\partial y}P_i]d\Omega - \frac{1}{\alpha^2}\int_{\Omega} N_{rj}\sum N_{rj}\, d\,\Omega\ddot{P}_i + \int_{\Gamma} N_{rj}\sum\frac{\partial N_{ri}}{\partial n}d\Gamma P_i = 0 \quad (3.25)$$

In which *I* varies from 1 to total number of nodes and ***Γ*** represents the boundaries of the fluid domain. The last term of the above equation may be written as

$$B=\int_{\Gamma} N_{rj}\frac{\partial P}{\partial N} \quad (3.26)$$

The whole system of equation (3.25) may be written in a matrix form as

$$(\overline{EE})\ddot{\overline{P}} + (GG)\overline{P} = \overline{F} \quad (3.27)$$

Where,

$$\overline{EE} = \frac{1}{\alpha^2}\sum\int_{\Omega} N_r^T N_r d\Omega \quad (3.28)$$

$$GG=\sum \int_{\Omega} [\frac{\partial N_r^T}{\partial x}\frac{\partial N_r}{\partial x} + \frac{\partial N_r^T}{\partial y}\frac{\partial N_r}{\partial y}]d\Omega \quad (3.29)$$

$$F=\sum \int_{\Gamma} N_r^T \frac{\partial P}{\partial n} d\boldsymbol{\Gamma} = \bar{F}_I + \bar{F}_{II} + \bar{F}_{III} \quad (3.30)$$

Here the subscript *I*, *II* and *III* stands for different surface conditions. For surface wave, the equation (3.21) may be written in finite element form as

$$\bar{F}_I = -\frac{1}{g} S_f \ddot{\bar{P}} \quad (3.31)$$

In which,

$$S_f=\sum \int_{\Gamma f} N_r^T N_r d\boldsymbol{\Gamma} \quad (3.32)$$

At the surface *II*, if $\{a\}$ is the vector of nodal acceleration of generalized coordinates, $\{F_{II}\}$ may be expressed as

$$F_{II} = -\rho_f R_{II} \bar{a} \quad (3.33)$$

In which,

$$S_{II} =\sum \int_{\Gamma_{11A}nd^{1v}} N_r^T N_r d\Gamma \quad (3.34)$$

At surface III

$$\bar{F}_{III} = 0 \quad (3.35)$$

After substitution all terms the equation (3.27) becomes

$$(EE)\ddot{\bar{P}} + (AA)\dot{\bar{P}} + (GG)\bar{P} = \bar{F}_r \quad (3.36)$$

Where,

$$EE = \overline{EE} + \frac{1}{g} S_I \quad (3.37)$$

$$\bar{F}_r = -\rho_f S_{II} \bar{a} - \rho_f S_{IV} \bar{a} \quad (3.38)$$

For any given acceleration at the fluid structure interface, the equation (3.26) is solved to obtain the hydrodynamic pressure within the fluid.

3.3 Computation of Velocity and Displacement of Fluid

The accelerations of the fluid particles can be calculated after computing the hydrodynamic pressure in reservoir. The velocity of the fluid particle may be calculated from the known values of acceleration at any instant of time using Gill's time integration scheme (Gill, 1951), which is a step-by-step integration procedure based on Runge-Kutta method (Ralston and Wilf, 1965). This procedure is advantageous over other available methods as (i) it needs less storage registers; (ii) it controls the growth of rounding errors and is usually stable and (iii) it is computationally economical. At any instant of time *t*, velocity will be

$$V_t = V_{t-\Delta t} + \Delta t \dot{V}_t \tag{3.39}$$

Velocity vectors in the reservoir may be plotted based on velocities computed at the Gauss points of each individual point. Similarly, the displacement of fluid particles in the reservoir, *U* at every time instant can also computed as

$$U_t = U_{t-\Delta t} + \Delta t V_t \tag{3.40}$$

3.4 Time History Analysis of dynamic equilibrium equation

Dynamic equilibrium equation of fluid can be expressed as

$$(EE)\bar{\bar{P}} + (AA)\bar{\dot{P}} + (GG)\bar{P} = \bar{F}_r \tag{3.41}$$

In a linear dynamic system, these values remain constant throughout the time history analysis. The force vector is given byF_r. To obtain the transient response at time t_N the time axis can be discretized into *N* equal time intervals ($t_N = \sum_{i=1}^{N} j\Delta t$). The choice of method for time-history analysis is strongly problem dependent. Various direct time integration methods exist for time history analysis that are expedient for structural dynamics and wave propagation problem. Amongst these, the Newmark family of method is most popular and is given by

$$P_{j+1} = P_j + \Delta t \dot{P}_j + \frac{\Delta t^2}{2}[(I - 2\gamma)P_j + 2\gamma \ddot{P}_{j+1}. \tag{3.42}$$

$$\dot{P}_{j+1} = \dot{P}_j + \Delta t[(1-2\gamma)]\ddot{P}_j + \gamma\ddot{P}_{j+1}] \quad (3.43)$$

Here ɣ and γ are chosen to control stability and accuracy. It is evident from the literature that the integration scheme is unconditionally stable if $2ɣ \geq \gamma \geq 0.5$.

3.4.1 Stability Analysis of Newmark Method

The aim of the numerical integration of time in the finite element system equilibrium equations is to approximate the actual dynamic response of the system under consideration. Stability of an integration scheme implies that the initial conditions for the equations with a large value of $\Delta t/T$ must not be amplified artificially. In a stable scheme, there is no abrupt increase of any errors in displacements, velocities and accelerations at time *t*, due to rounding off during computation. Stability is acquired if the time step chosen is small enough to integrate accurately the response in the highest frequency component. It is important to optimize the size of the time step, so as to obtain accuracy but at the same time to avoid an increase in computational cost.

3.4.2 Accuracy Analysis of Newmark Method

In a practical analysis, the choice of the integration operator depends on the cost of solution that can be determined by the number of time step required in the integration. For a conditionally stable algorithm such as central difference, the time steps for a given time range considered is determined by the critical time step Δt_{cr} and not many choices are available. The errors in the integration may be measured in terms of period elongation and amplitude decay. When the time step to period ratio is larger, the various integration methods exhibit quite different characteristics. For a given $\Delta t/T$, the Wilson-θ method with θ = 1.4 introduces less amplitude decay and period elongation than the Houbolt method, and the Newmark average acceleration method introduces only period elongation and no amplitude decay. If the Newmark constant average acceleration is employed, the high frequency response is retained in the solution. It is observed that the method corresponding to γ = 0.5 and ɣ= 0.25 has the most desired stability. Therefore, in the present work, the dynamic equilibrium equations are solved using the values of γ and ɣ as 0.5 and 0.25 respectively.

CHAPTER 4

RESULTS AND DISCUSSIONS

4.1 Validation of the Proposed Algorithm.

In order to validate the proposed algorithm, a bench marked problem is solved and results are compared with the results obtained by Virella et al. (2008). The geometric and material properties of the tank are considered as follows: height of water in the tank = 6.10 m, length of tank = 30.5 m, so that ratio of height to length (h/L) = 0.2, density of water = 983 kg/m^3, pressure wave velocity = 1451 m/s. Here, the interaction of fluid with in the tank and tank walls is neglected and the fluid is discretized by 5 ×10 (i.e., N_h= 5 and N_v = 10). The first three natural time periods of the tank fluid are listed and compared with those values obtained by Virella et al. (2008) in Table 4.1. The tabulated results show the accuracy of the present method.

Table 4.1 First three natural time period of the tank fluid

Mode number	Natural Time period in sec	
	Present Study	Virella et al. (2008)
1	8.45	8.38
2	3. 95	3.70
3	2.90	2.78

4.2 Selection of Time Step

Since the compressibility effect of water is included, the results are quite sensitive to the time step in Newmark's integration technique. In order to obtain a suitable time step, tank with following properties is considered. Water depth (h) = 2.0 m, length of tank (L) =1.0 m acoustic speed (α) = 1439 m/sec, mass density of water (ρ_f) = 1000 kg/m^3. The study is carried out for three different

exciting frequencies, *TC/h* as 200, 900 and 4000, (*T* is time period of excitation) with amplitude of 10.0g. Here, the fluid domain is discretized by 5 × 10 (i.e., N_h = 5 and N_v = 10) (Fig. 4.1) and the base of the tank is considered to be rigid. The maximum pressure coefficient ($C_p = p/\rho * Amp * h$) for different number of time step (N_t) at different exiting frequencies are summarized in Table 4.2. It is observed from the tabular results that the developed hydrodynamic pressure for different values of *TC/h* is converged for values of N_t= 32. Thus, the time step (Δt) for the analysis of water tank is adopted as *T*/32 for all the case unless it is mentioned.

Table 4.2 Convergence of hydrodynamic pressure coefficients (C_p) for different time steps

N_t	*TC/h*= 200	*TC/h*= 900	*TC/h*= 4000
8	0.6055	8.6843	2.2265
16	0.6245	9.3560	2.4001
24	0.6250	9.8790	2.4187
32	0.6253	9.8836	2.4194
64	0.6253	9.8836	2.4194
128	0.6253	9.8836	2.4194

4.3 Selection of Suitable Mesh Size

To obtain a suitable mesh size, tank with following properties is considered. Water depth (*h*) = 1.6 m, length of tank (*L*) =0.8 m acoustic speed (α) = 1440 m/sec, mass density of water (ρ_f) = 1000 kg/m^3. The study is carried out for an exciting frequencies of *TC/h* =4000 with amplitude of 1.0 g. The maximum pressure coefficient ($C_p = p/\rho * Amp * h$) for different mesh size are summarized in Table 4.3. From Table 4.3 it is observed that the maximum hydrodynamic pressure is converged when the horizontal division (N_h) is equal or higher than 4 and the ratio of vertical division to horizontal division (N_v/N_h) is equal to 1.0. However, for further numerical study, N_h is consider as 4 and the higher value (Fig 4.1). The values N_h and N_v are mention in respective examples.

Table 4.3 Convergence of hydrodynamic pressure coefficients (C_p) for different mesh size

Mesh Size ($N_h \times N_v$)	N_v/N_h	Pressure coefficient $(P/(a\rho d))$
(1 ×1)	1	1.5773
(1 ×2)	2	1.8654
(2×1)	0.5	1.6293
(2 ×2)	1	1.9792
(3 ×1)	0.33	1.9108
(3 ×2)	0.67	1.9861
(3 ×3)	1	2.0568
(4 ×2)	0.5	2.0761
(4 ×3)	0.75	2.1274
(4 ×4)	1	2.2792
(4 ×6)	1.5	2.2792
(6 ×6)	1	2.2792

4.4 Analysis of rectangular tanks

In this section, the convective responses of tank with different size are studied. The material properties for water with in the tank are follows: acoustic speed in water (α) = 1440 m/sec, mass density of water (ρ_f) = 1000 kg/m^3. In the present study, tank walls and the tank bottom are considered as rigid. The water in the tanks is discretized by 10 × 10 (i.e., N_h = 10 and N_v = 10) as obtained in the section 4.3. Similarly, the time step for time history analysis is considered as T/32 when the excitations are considered to be harmonic.

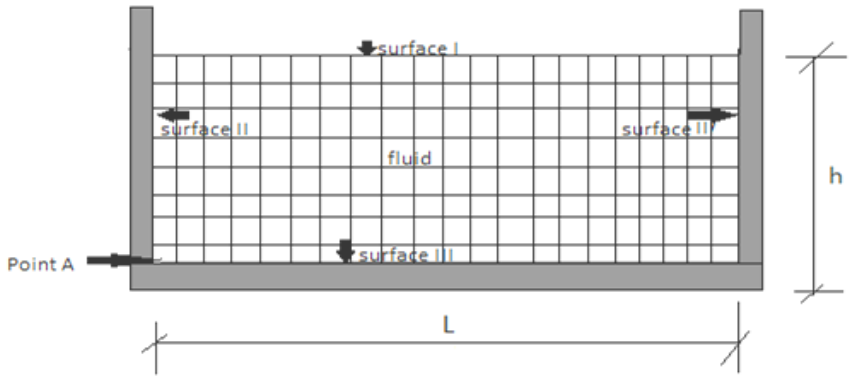

Fig. 4.1 A typical finite element meshing of water

4.4.1Size effect on convective time period of rectangular water tanks

In order to study the influences of size on convective time period of rectangular water tanks, the length of tanks is considered as 30.5m. However, tanks height is considered to be different values. Fig. 4.2 shows the variation of first three convective time periods with different height to length ratios (*h/L*). From the figure it is clear that all three convective time periods decrease with the increase of *h/L* initially ($C_c=T_c/(\sqrt{(L/g)}$, *Tc* is time period*)*. However, after certain value of *h/L* convective time period become almost constant. The effect of *h/L* ratio is prominent in case of first fundamental time period. However, the effect is negligible small for third fundamental time period.

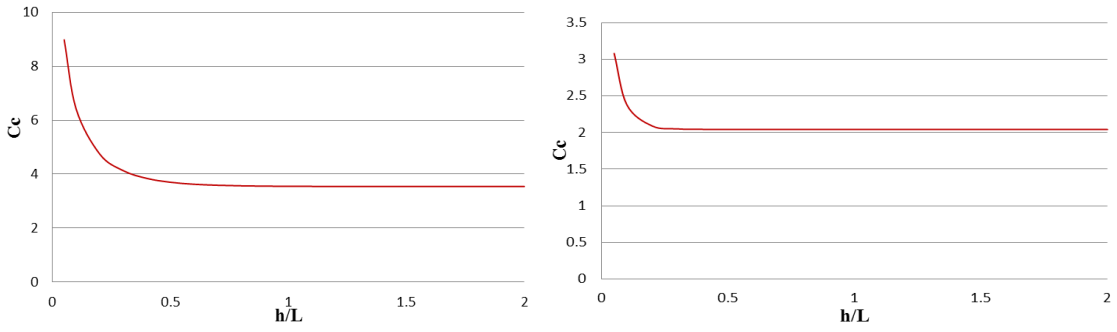

(a) First (b) Second

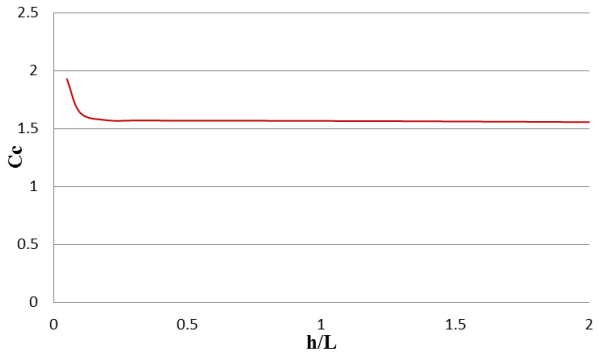

(c) Third

Fig. 4.2 Variation of convective time period with the sizes of water tank

4.4.2 Convective Responses of tanks with different height of tanks

In this section, the responses of tank with different height are studied. The material properties for water with in the tank are follows: acoustic speed in water (α) = 1440 m/sec, mass density of water (ρ_f) = 1000 kg/m^3. In the present study, tank walls and the tank bottom are considered as rigid. The water is discretized by 10 × 10 (i.e., N_h = 10 and N_v = 10) as obtained in the section 4.3. Similarly, for time history analysis the time step is considered as T/32 (section4.2). Here, the length of tanks is considered to be 25m and different values such as 5m, 12.5m, 25m, 37.5m and 50m are considered as height.

The responses of tanks in term of hydrodynamic pressure, sloshed displacement and velocity distribution are determined for sinusoidal acceleration of frequency equal to the fundamental frequency of fluid within tank. The convective hydrodynamic pressure at free surface is more compare to the hydrodynamic pressure at other locations and it is interesting to see that the convective hydrodynamic pressure at free surface is constant for all height of tanks (Fig. 4.3a). However, the convective hydrodynamic pressure at bottom (Fig. 4.3c) and mid height (Fig. 4.3b) of tank wall varies with the height of tanks. The greater hydrodynamic pressure is observed for comparatively narrow water tank. The distribution of pressure co-efficient ($Q_{cw}=P_{cw}/a\rho gL$, P_{cw} is convective pressure on wall) is also plotted for various heights of tank (Fig. 4.4). The pattern of distributions changes with the height of tanks. The distribution is parabolic in nature for comparatively lower height. Again, the pressure coefficient decreases with the increase of height of tank. The convective hydrodynamic pressure at the base ($Q_{cb}=P_{cb}/a\rho gL$, P_{cb} is convective pressure

on base slab) of tanks also depends on height of the tanks (Fig.4.5). The hydrodynamic pressure increases with the decrease of height and it is interesting to see that the convective hydrodynamic pressure at the midpoint of base slab is zero for all heights. The sloshed displacement along the free surface of the tanks fluid is also plotted for various height of tanks in Fig. 4.6. This figure depicts that 50% of fluid present in tanks goes up and remaining 50% of goes down with respect to its initial position. The maximum sloshing occurs near the tanks wall and the sloshing is almost zero near the midpoint of the free surface. It is further noted that the displacement of free surface does not depend on the tanks height which support the variation of convective hydrodynamic pressure at free surface with the height of tanks wall. The velocity distribution within the water in the tank is plotted for various height of the water in Fig. 4.7. From this figure it is clear that the disturbance is greater when the tank height is 5m and this disturbance gets reduced continuous as the height increases. For tank of height 50m, the disturbance is concentrated at the free surface of the water and water particles near the bottom slab of tank follows almost smooth distribution pattern (Fig.4.7e). Contour plot of convective hydrodynamic pressure in Fig. 4.8 also support the distribution of velocity within the tanks. For tank of height 5m, hydrodynamic pressure distributed all over the tank. However, for tank height of 37.5m and 50m the convective hydrodynamic pressure is distributed only at the upper part of the tank and the hydrodynamic pressure is almost zero after a certain depth (Fig.4.8d-e).

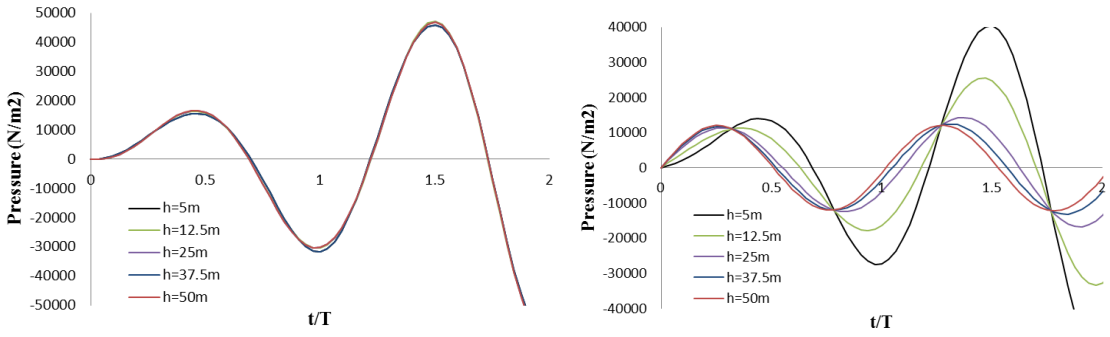

(a) (b)

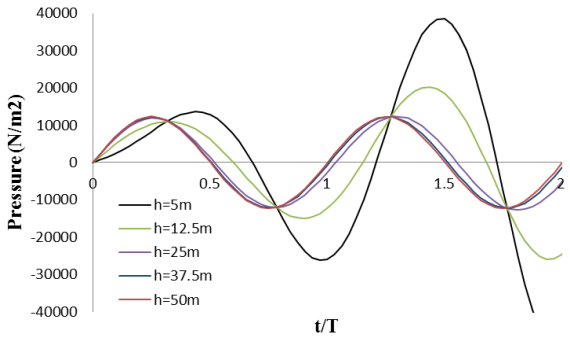

(c)

Fig.4.3 Variation of convective hydrodynamic pressure a) at Free surface b) at mid height of wall c) at bottom of wall

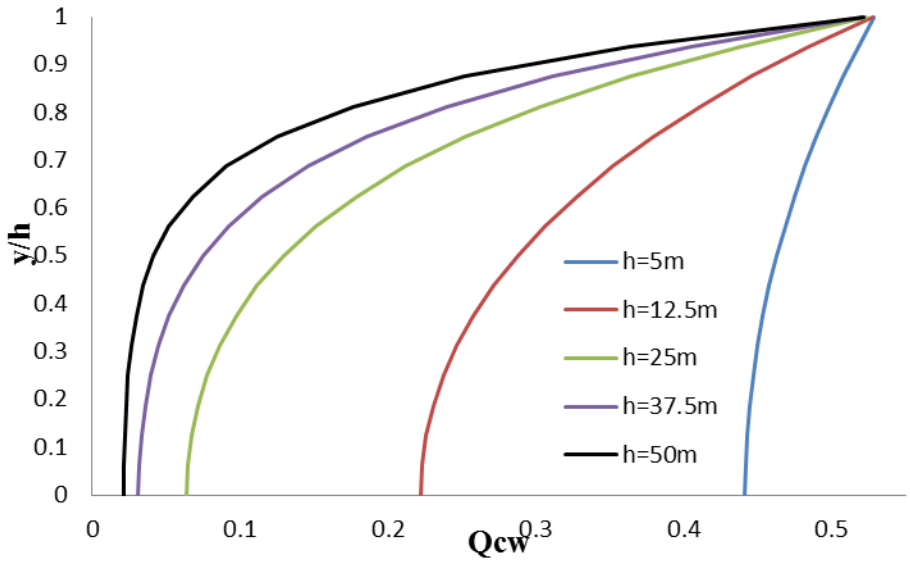

Fig.4.4 Distribution of convective hydrodynamic pressure along tanks wall

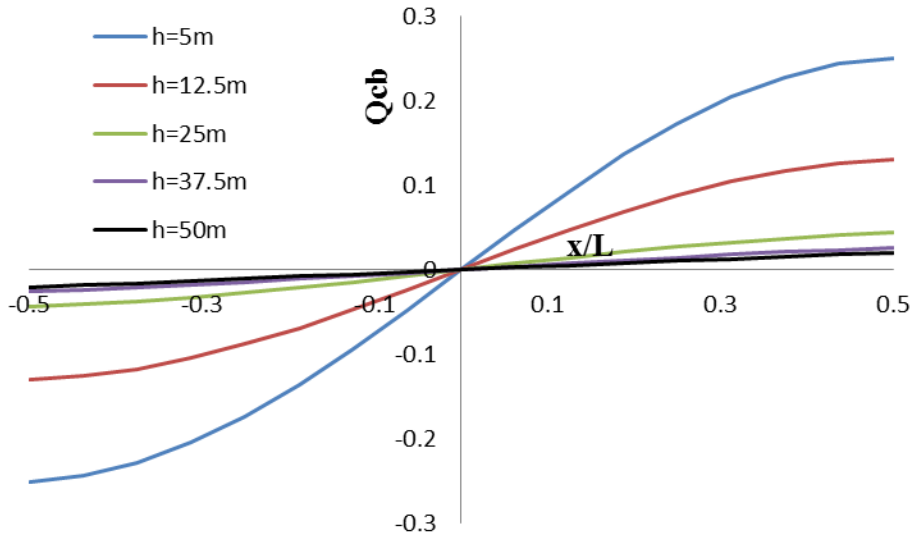

Fig.4.5 Distribution of convective hydrodynamic pressure along base of tanks

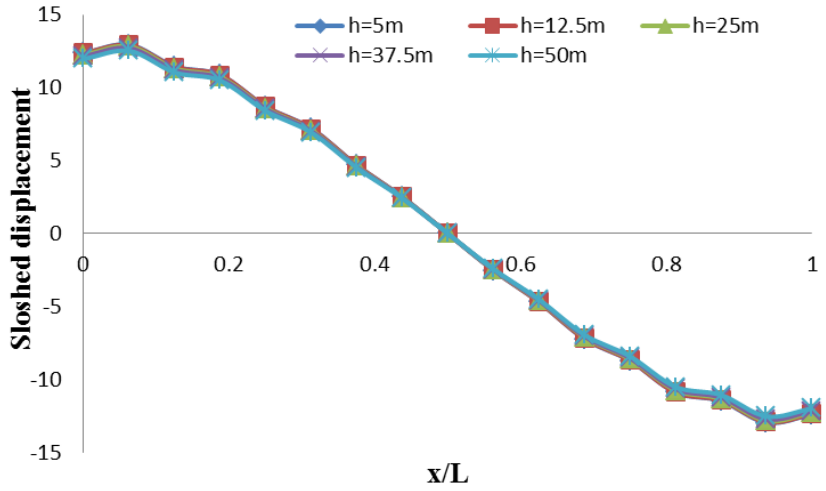

Fig.4.6 Variation of sloshed displacement with the height of tanks wall.

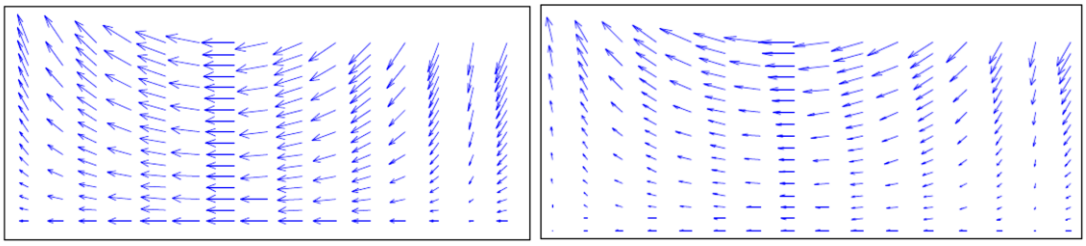

(a) h=5m (b) h=12.5m

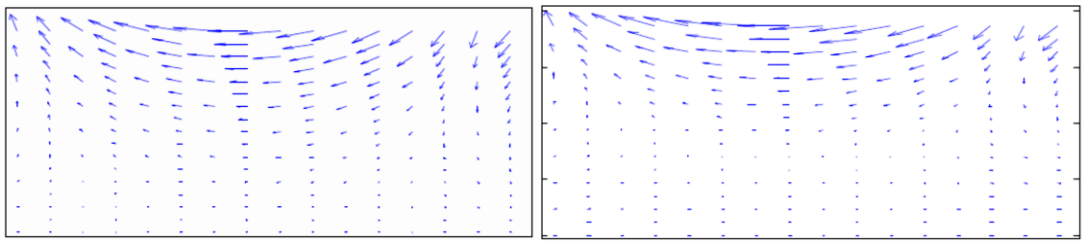

(c) h=25m (d) h=37.5m

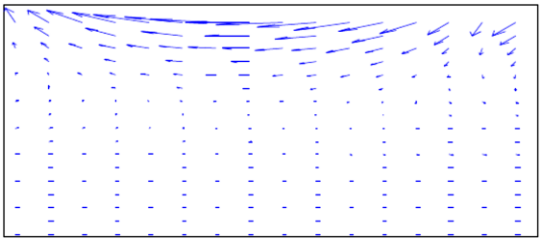

(e) h=50m

Fig.4.7 Velocity distribution within the fluid for different heights of tank wall

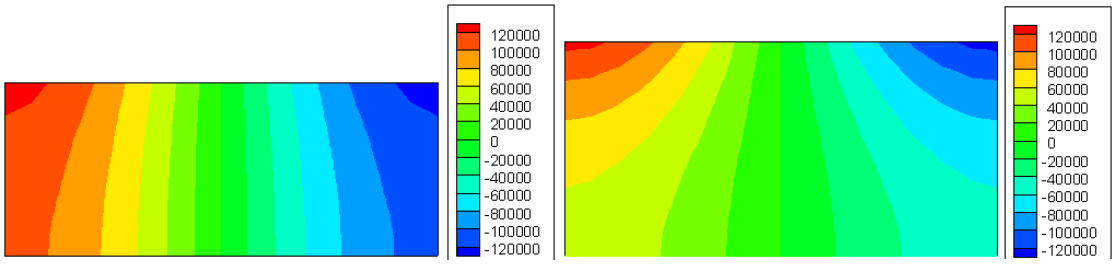

(a) h=5m (b) h=12.5m

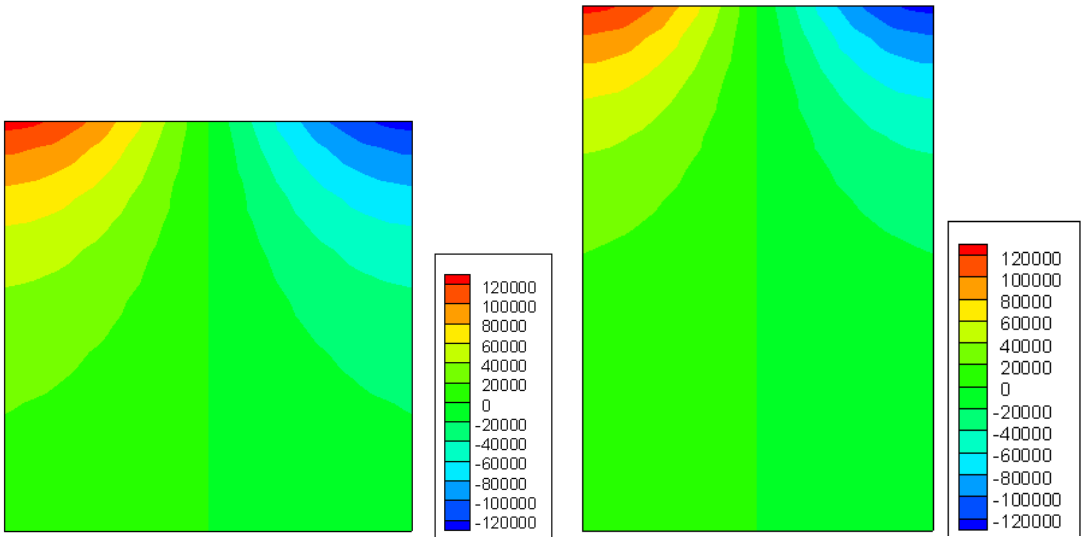

(c) h=25m (d) h=37.5m

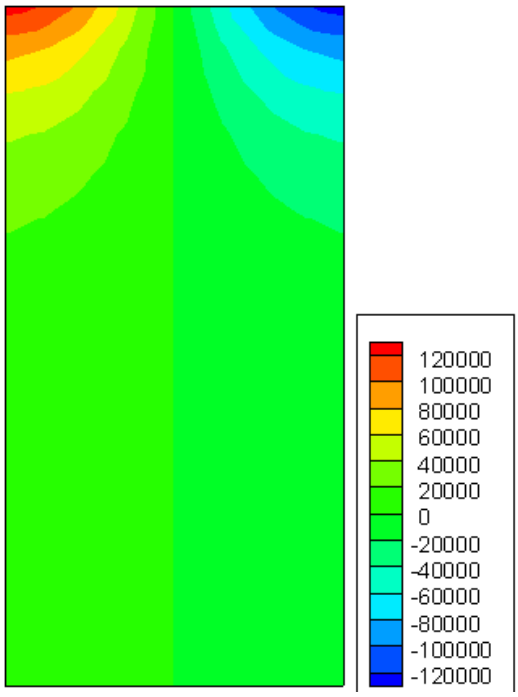

(e) h=50m

Fig.4.8 Contour plot of hydrodynamic pressure for various tank heights

4.4.3 Convective Responses of tanks with different length of tank

The responses of tank with different length are presented here. The properties for water are as considered in section 4.4.1.Here also tank walls and the tank bottom are considered as rigid and the fluid is discretized by 10 × 10. The height of tanks is considered to be 10m and different values such as 5m, 6.667m, 10m, 20m and 50m are considered as length. The frequency of the external excitation is considered to be the fundamental frequency of the fluid within the tanks.

The convective hydrodynamic pressure at different location along the tank wall is plotted in Fig.4.9. From this figure it is clear that the convective hydrodynamic pressure all locations such as at free surface, at the mid height of tank wall and at the base of tanks depends on the length of the tank and the magnitude of the pressure increases with the increase of tanks length. This increase is more for comparatively higher tank length. The convective hydrodynamic pressure has highest magnitude when it is compared to the hydrodynamic at other two locations. The convective hydrodynamic pressure at the free surface is experienced more enhanced value with the increase of length of the

tank. The variation of convective hydrodynamic pressure along tank wall and the base of tank are plotted for different tank lengths in Fig.4.10 and Fig.4.11 respectively. The variation of the pressure along tanks wall and the base of tank are almost similar to the respective variation of hydrodynamic pressure for tanks with fixed height. However, in this case, the pressure increases with the increase of tank length. The displacement of fluid at free surface for different lengths of tank is plotted in Fig. 4.12. This figure depicts that the elevation of free surface depends on the length of tanks. The smallest vertical displacement occurs for length equal to 5m.The sloshing of free surface increases continuously from the smallest length to highest length of tank. The velocity distribution within the water in the tank not only depends on the tank height but also on the length of the tank. However, the disturbance due to the external excitation will be more for comparatively longer tank (Fig.4.13). In this case, the convective hydrodynamic pressure is more for comparatively large tank and it is distributed all over the tank (Fig.4.13). However, the hydrodynamic pressure is distributed only near the free surface when the length of the tank is 5m or 6.667m (Fig.4.13a and Fig.4.13b).

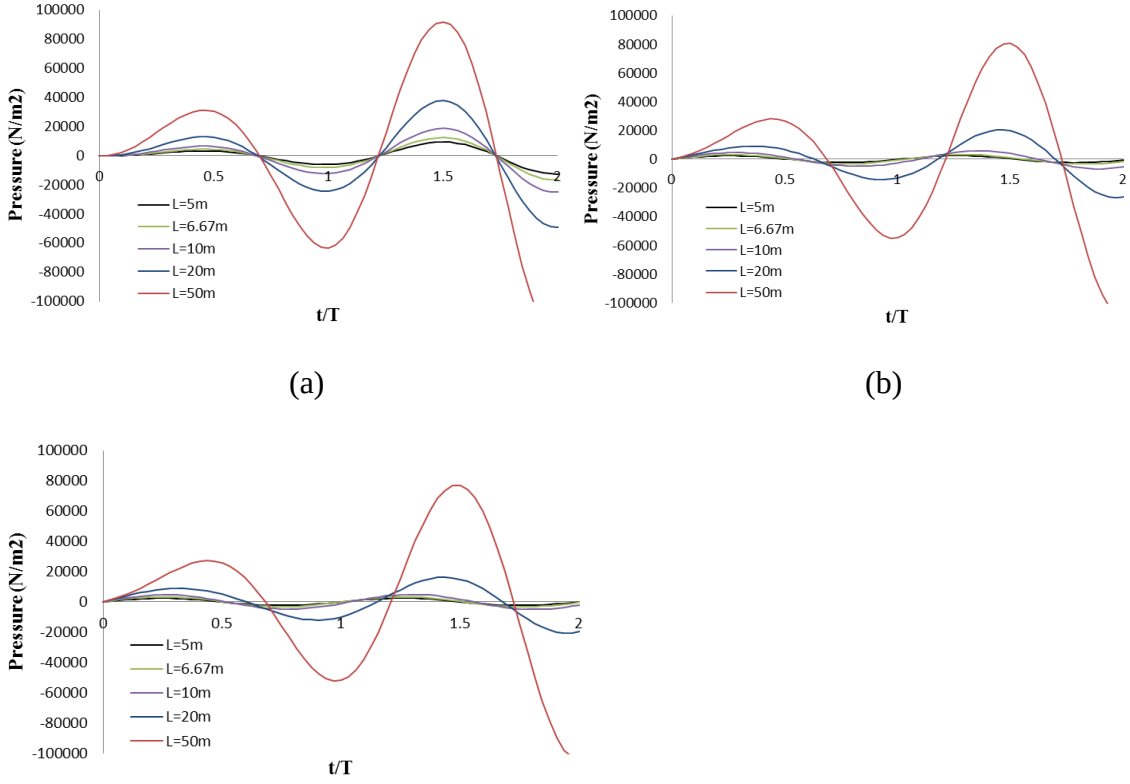

Fig.4.9 Variation of convective hydrodynamic pressure for various lengths of tank a) at Free surface b) at mid height of wall c) at bottom of wall

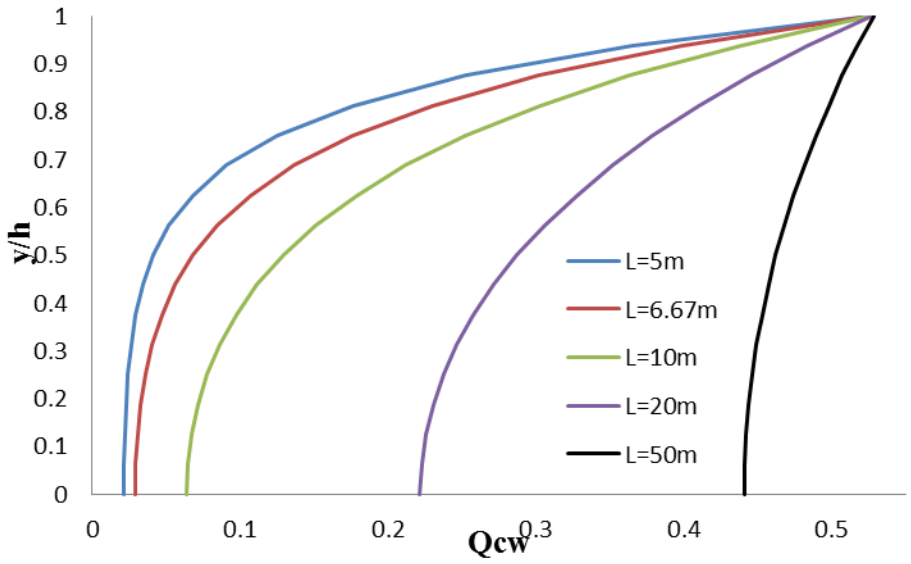

Fig.4.10 Variation of convective hydrodynamic pressure along tank wall for various lengths of tank

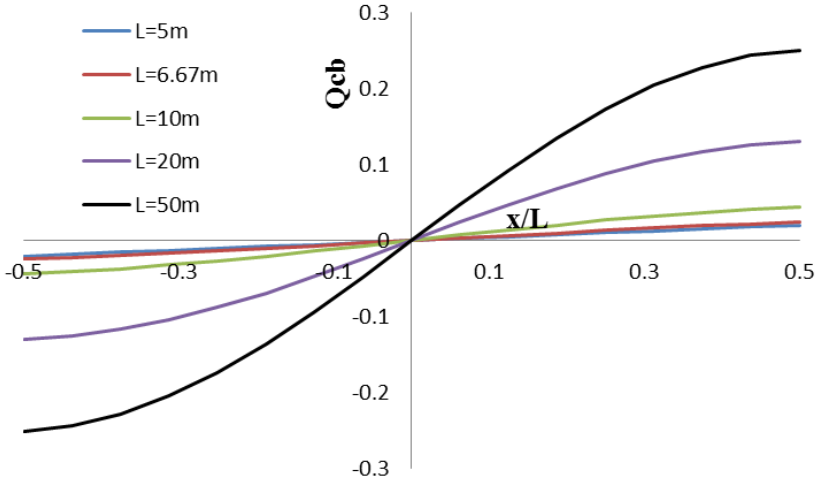

Fig.4.11 Distribution of convective hydrodynamic pressure along base of tank for different lengths of tank

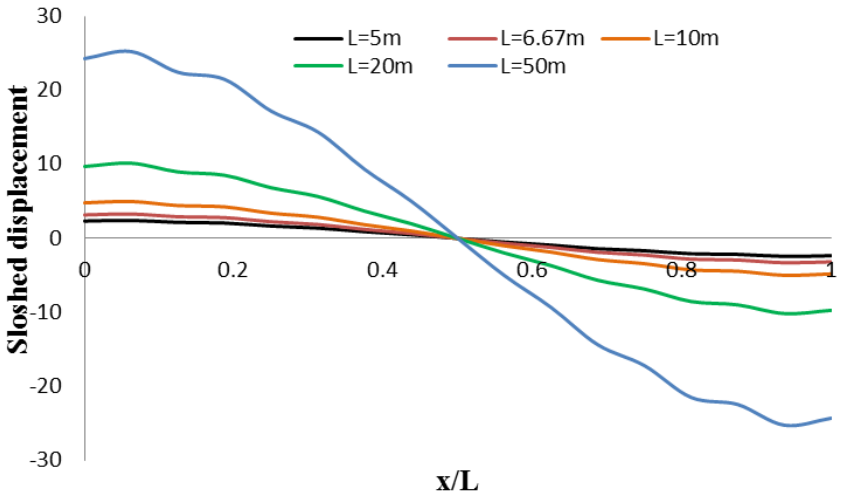

Fig.4.12 Variation of sloshed displacement with the length of tank

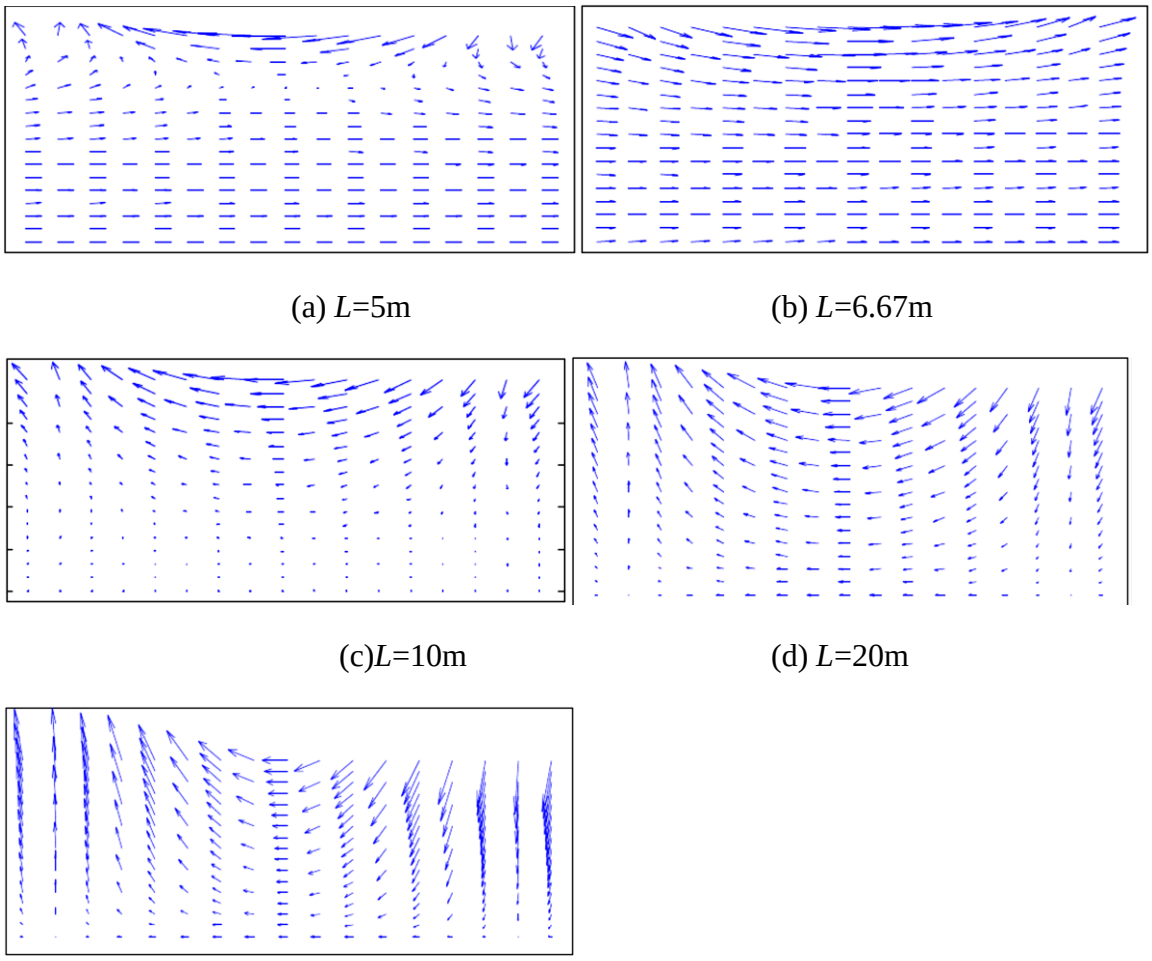

(a) *L*=5m (b) *L*=6.67m

(c)*L*=10m (d) *L*=20m

(e) *L*=50m

Fig.4.13 Velocity distribution within the fluid for different lengths of tank

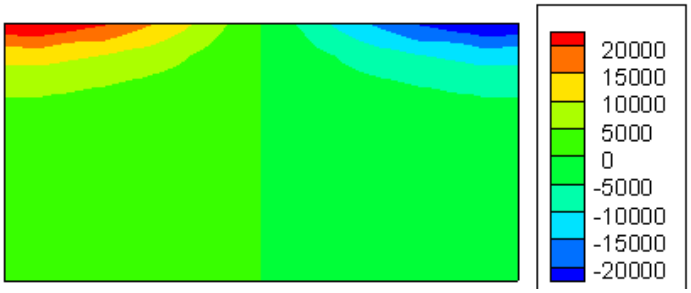

(a) L=5m

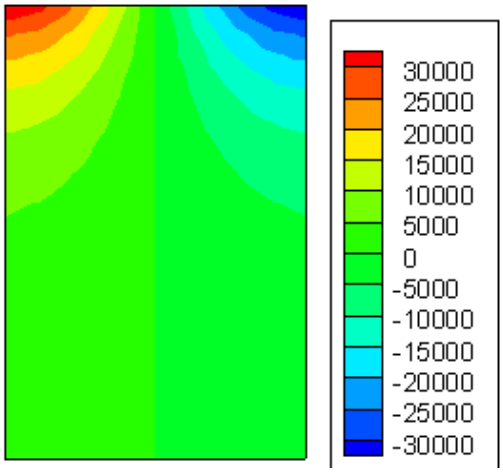

(b) L=6.67m

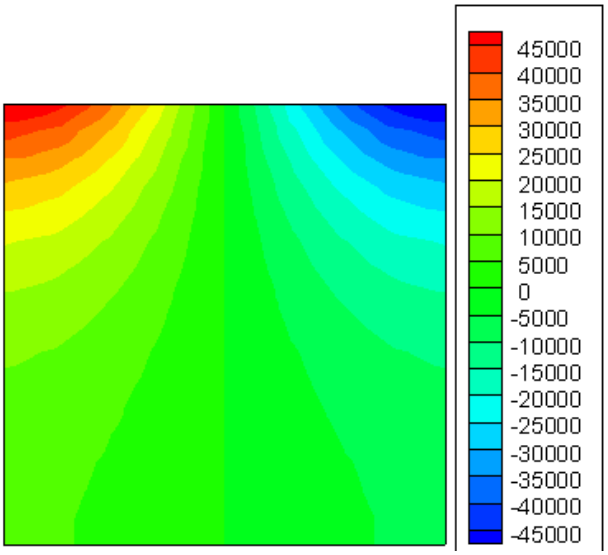

(c) L=10m

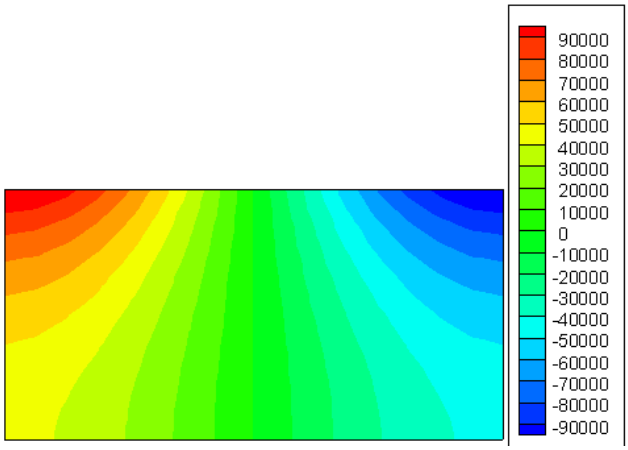

(d) L=20m

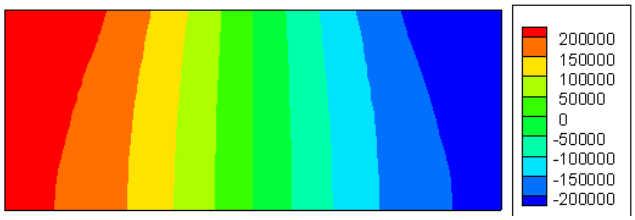

(e) L=50m

Fig.4.14 Contour plot of hydrodynamic pressure for various tank heights

CHAPTER 5

CONCLUSIONS

The characteristics of convective responses of rectangular water tanks are studied. The water in the tank is considered to be linearly compressible. A pressure based finite element method is used to simulate the water in the tanks and tank walls are considered to be rigid. The advantages of the pressure based is in the computational aspect compared to the velocity potential and the displacement based modeling, as the number of unknown per node is only one.

The hydrodynamic pressure on the tank walls is considered to the main aspect during design of tanks. In the present study, the convective responses are determined for different sizes of rectangular tanks.

The convective time period of tank water decreases with the increase of the height to length ratio. This variation is different for different time periods. The effect of height to length ration is more in case of first fundamental time period and this effect decreases subsequently for higher time periods.

The convective hydrodynamic pressure within tank depends on height of tanks. The convective hydrodynamic pressure at base slab and at the mid height of tank wall has higher value for comparatively narrow tank. However, the convective hydrodynamic pressure at the free surface is independent of tank height. The extend of disturbance of fluid in tank due to external excitation depends on the tank height. The amount of water excited with the external excitation increases with the increase of height of tank. However, the sloshed displacement at the free surface remains constant for different heights of tank.

The convective hydrodynamic pressure at free surface as well as at mid height of tank wall and the base of tank depends on tank length. This pressure at all locations increases with the increase of tank length. For the case of different tank length, the extend of disturbance within the tank increases with the increase of tank length. The elevation of frees surface also depends on tank length. For comparatively lower tank length, the free surface experienced lesser elevation at free surface.

5.1 Future Scope of Work

The present work is an investigation of the convective response of rectangular fluid container. There are certain other aspects that may be considered for further research:

- The present study is limited to the finite element analysis of fluid domain only. The study may be further extended considering flexibility of tank walls and fluid-structure interaction.
- In the present case, baffle is not considered. In future, the study may be extended considering the baffle within the tanks.
- The present problem may be extended to 3-dimensional form with and without fluid-structure interaction.
- The analysis may also be performed for cylindrical and other types of tank.
- Non-linear wave theory may be used to simulate the water or other fluid motion within the tank.

REFERENCES

Adhikary R. and Mondal K.K. (2018), "The dynamic analysis of water storage tank with rigid block at bottom", Ocean Systems Engineering, 8, No. 1, 57-77.

Boroomand B, Bazazzadeh S. and Zandi S.M. (2016), "The use of Laplace's equation for pressure and a mesh-free method for 3d simulation of nonlinear sloshing in tanks". Ocean Engineering, 122, 54–67.

Choun Y.S. and Yun C.B. (1996) "The effects of a bottom-mounted rectangular block of arbitrary size and location on the sloshing frequencies and mode shapes of the fluid in rectangular rigid tanks". Computers and Structures, 61, No. 3, 401-413.

Chen Y.G, Djidjeli K. and Price W.G. (2009), "The numerical simulation of liquid sloshing phenomena in partially filled containers." Computers & Fluids, 38 (2009), 830–842.

Cho I.H and Kim M.H. (2016), "The effect of dual vertical porous baffles on sloshing reduction in a swaying rectangular tank". Ocean Engineering, 126, 364–373.

Chaudhari1 K., Bhilare B.L. and Patil G.R. (2017), "The dynamic response of circular water tank with baffle walls." International Research Journal of Engineering and Technology, 04, No.1, 2094-2099.

Cho I.H, Choi J.S. and Kim M.H. (2017), "The Sloshing reduction in a swaying rectangular tank by a horizontal porous baffle". Ocean Engineering, 138, 23–34.

Eswaran M, Saha U.K. and Maity D. (2009), "The effect of baffles on a partially filled cubic tank. In this paper, sloshing waves were analyzed for baffled and un-baffled tanks". Computers and Structures, 87 (2009), 198–205.

Faltinsen O.M and Timokha A.N (2011), "The natural sloshing frequencies and modes in a rectangular tank with a slat-type screen". Journal of Sound and Vibration, 330, 1490–1503.

Gill S (1951) "A process for the step-by-step integration of differential equations in an automatic digital computing machine", Proceedings of the Cambridge Philosophical Society, 47, 96-108.

Grotle E.L, Bihs. H. and Vilmar E. (2017), "The experimental and numerical investigation of sloshing under roll excitation at shallow liquid depths". Ocean Engineering, 138, 73–85.

Hasheminejad S.M and Aghabeigi M (2011), "The transient sloshing in half full horizontal tank under lateral excitation". Journal of Sound and Vibration, 330, 3507–3525.

Idelsohn S, Torrecilla M.M. and Onate E. (2009), "The Multi-fluid flows with the Particle Finite Element Method". Comput. Methods Appl. Mech. Engg, 198, 2750–2767.

Iranmanesh A. and Passandideh-Fard M. (2017), “2D numerical study on suppressing liquid sloshing using a submerged cylinder”. Ocean Engineering, 138, 55–72.

Javanshir A, Elahi R. and Passandideh-fard M. (2013), “The numerical simulation of liquid sloshing with baffles in the fuel container”. Iranian Aerospace Society Conference, AERO2013-17469.

Jung J.H, Yoon H.S. and Lee C.Y. (2015), “The effect of natural frequency modes on sloshing phenomenon in a rectangular tank”. International Journal of Naval Architecture and Ocean Engineering, 7,580-594

Lin L, Sheng C.j, Ming.z. And Guo Q.T (2015), “The two dimensional viscous numerical simulation of liquid sloshing in rectangular tank with/without baffles and comparison with potential flow solution”. Ocean Engineering, 108, 662–677.

Liu D, Tang W, Wang J, Xue H. and Wang K. (2017), “The modelling of liquid sloshing using CLSVOF method and very large eddy simulation”. Ocean Engineering, 129, 160–176.

Mitra S. and Sinhamahapatra K.P. (2008), “The 2D simulation of fluid-structure interaction using finite element method.” Finite Element analysis and Design, 45, No.1, 52-59.

Ming P.J. and Duan W.Y. (2010), “The numerical simulation of sloshing in rectangular tank with VOF based on unstructured grids”. Journal of hydrodynamics, 22, No.6, 856-864.

Miao Y. and Wang S. (2014), “The Small amplitude liquid surface sloshing process detected by optical method”. Optics Communications, 315, 91–96.

Nan. M, Junfeng L. and Tianshu W. (2017), “the equivalent mechanical model of large-amplitude liquid sloshing under time-dependent lateral excitations in low-gravity conditions”. Journal of Sound and Vibration, 386, 421–432.

Pal N.C., Bhattacharyya S.K. and Sinha R.K. (2001) “Experimental Investigation of Slosh Dynamics of Liquid-filled Containers”. Experimental Mechanics, 41, No-1 63-69.

Pal P. and Bhattacharyya S.B (2010), “The Sloshing in partially filled liquid containers— Numerical and experimental study for 2-D problems”. Journal of Sound and Vibration, 329, 4466–4485.

Ralston A. and Wilf, H.S. (1965) Mathematical Models for Digital Computers, Wiley, New York.

Rebouillat S. and Liksonov D. (2010), “The fluid–structure interaction in partially filled liquid containers”. Computers & Fluids, 39, 739–746.

Su Y. and Liu Z.Y. (2016), “The Numerical model of sloshing in rectangular tank based on Boussinesq type equations”. Ocean Engineering, 121, 166–173.

Sufyan M, Ngo L.C and Choi H.G. (2017), “The dynamic adaptation method based on unstructured mesh for solving sloshing problems”. Ocean Engineering, 129, 203–216.

Tung Y. (1994) “The dynamic characteristics of rigidly supported upright circular cylindrical tanks containing two different liquids.” J. Struct. Eng. - ASCE. 120, No.3, 618-636.

Takabatake D, Sawada S, Yoneyama and Miura M. (2008), “The effect of splitting wall as sloshing reduction device in a cylindrical tank”. The 14th World Conference on Earthquake Engineering October 12-17, Beijing, China.

Virella J.C., Prato C.A and Godoy L.A (2008). “Linear and nonlinear 2D finite element analysis of sloshing modes and pressures in rectangular tanks subject to horizontal harmonic motions”, J. of Sound and Vibration, 312, No.23, 442-460.

Vakilaadsarabi A. and Miyajima M. (2012), “The sloshing of water reservoirs and tanks due to long period and long duration seismic motions.”15 WCEE, LISBOA, 2012.

Wei W, Junfeng L. and Tianshu .W (2008), “The modal analysis of liquid sloshing with different contact line boundary conditions using FEM”. Journal of Sound and Vibration, 317, 739–759.

Wu C.H, Faltinsen O.M. and Chen B.F. (2012), “The numerical study of sloshing liquid in tanks with baffles by time-independent finite difference and fictitious cell method”. Computers & Fluids, 63, 9–26.

Xue M.A. and Lin P. (2011), “The numerical study of ring baffle effects on reducing violent liquid sloshing”. Computers & Fluids, 52, 116–129.

Xue M.N, Zheng J, Lin P. and Yuan X. (2017), “The experimental study on vertical baffles of different configuration in suppressing sloshing pressure”. Ocean Engineering, 136,, 178–189.

Yuan C. and Xianlong J. (2010), “The dynamic response of flexible container during the impact with ground”. International Journal of Impact Engineering, 37, 999-1007.

Yu Y.M, Ma. N, Fan. C.M. and Gu. X.C. (2017), “The experimental and numerical studies on sloshing in a membrane-type LNG tank with two floating type baffle plates”. Ocean Engineering, 129, 217–227.

Zhang Y.X. and Wan D.C (2014), “Study of MPS (moving particle semi-implicit) method and level-set method for sloshing flows.” Journal of hydrodynamics, 26, No.4, 577-585.

Zhang H. and Wang Z. (2016), “The attitude control and sloshing suppression for liquid-filled spacecraft in the presence of sinusoidal disturbance”. Journal of Sound and Vibration, 383, 64–75.